A FIBER OPTIC LINEAR LINK FOR REMOTE APPLICATIONS

FABRICATION AND EVALUATION OF A LINEAR FIBER OPTIC DATA LINK POSSESSING AUTORANGING CAPABILITIES

BY

CHRISTOPHER MICHAEL LOOK, B.Sc.

A THESIS

Submitted to the School of Graduate Studies

in Partial Fulfilment of the Requirements

for the Degree

Master of Engineering

McMaster University

September 1980

Master of Engineering (1980)
(Engineering Physics)

McMaster University
Hamilton, Ontario

TITLE: Fabrication and Evaluation of a Linear Fiber Optic Data Link Possessing Autoranging Capabilities

AUTHOR: Christopher Michael Look, B.Sc. (Simon Fraser University)

SUPERVISOR: Dr. J.P. Marton

NUMBER OF PAGES: iv, 46.

ABSTRACT

The design and fabrication of a low cost optical communications link is described. The evaluation of this system shows that it can transmit bipolar analog signals in a bandwidth of 0 to 17 kHz with less than 0.1% non-linearity. Combined with an autoranging capability, the linear link is demonstrated to be useful for high accuracy remote data acquisiton.

ACKNOWLEDGEMENTS

I would like to thank my campus advisor, Dr. J.P. Marton for suggesting the project and his help in its completion, my present manager, Dr. J. Straus, for his active encouragement, T. Devenyi for his invaluable electronic assistance and G. Duck for his aid in the coupler fabrication. A special thanks goes to my wife, Debbie, who not only typed this project report, but whose active support enabled me to complete the project.

INTRODUCTION

The relatively recent realization of low loss optical fibers coupled with the emergence of compatible light sources and detectors has resulted in rapid development programs which have brought this technology from the laboratory into the field. Interest in fiber optics has been due primarily to the potential for low attenuation losses, very high data rates and high electro-magnetic noise immunity. These considerations have motivated telephone and cable television companies to play leading roles in this development. In common with any other infant technology, initial high system costs cause the widespread replacement of copper wires with optical fibers to be uneconomic at the present time. There are however, a large number of specialized tasks for which fiber optic technology is ideally and economically suited for even now. For example, the essentially infinite resistance of the glass fiber eliminates ground loops, electro-magnetic interference problems and, more generally, should be the choice when absolute electrical isolation is required, such as the monitoring of high voltages or for medical applications.

This report describes the design, construction and evaluation of a precision system for use in critical environments. Specifically, the system is a highly linear analog link consisting of two "black boxes" connected by an optical fiber. It is designed to produce an analog output voltage (V_{out}) at the "control" box which is linearly related to a voltage (V_{in}) applied to the remote unit. (More formally, $V_{out} = k \cdot V_{in}$ where k is a constant.) This relation is to be kept to within $\pm$ 0.1% (of full scale) from D.C. to 17 kHz. Moreover, the value of k should remain unchanged despite aging or temperature variations.

It is envisioned that such a linear link would be useful for remote data acquisition or monitoring of critical potentials in environments possessing strong electromagnetic noise sources. With these applications in mind, it is necessary that the remote unit have a sufficiently low power consumption that it could operate from either storage batteries or solar cells as well as more conventional power supplies.

As the system is aimed at several different applications, it must be able to adapt to a large range of input voltages on just a plug-in/turn-on basis. To increase its versatility the system will have a certain amount of "intelligence". In order to ensure maximum resolution of the monitored voltage the remote unit can automatically gain switch the applied voltage to provide a full scale output at the control unit. Certain signals near the gain switching frequency can play havoc with the autoranging. If for this, or any other reason, the autoranging facility is not desired, the operator can have the control unit itself communicate with the remote. It can order the remote to auto-range, have any selected fixed gain or even to multiplex data as required. Thus, just by a turn of a knob, the operator could change gain, get information (for example) on the ambiant temperature at the remote or the state of the remote's power supply and then leave the system in the autoranging mode.

Finally, the linear link is designed to operate over medium distances ($\sim$1 km). To minimize costs, only a single fiber is to be used to connect the control and remote units. To summarize, the objective of this project is to demonstrate the feasibility of an inexpensive low frequency, high linearity analog link. This link is to operate over distances up to a kilometer, be capable of battery operation and have minimum sensitivity to aging or temperature changes. To accommodate a large range of signals, it shall have a high impedance input and a low output impedance as well as having autoranging capabilities.

DESIGN CONSIDERATIONS

The dominant source of non-linearity in a well designed fiber optic link is the optical source.[1] Current state-of-the-art lasers can keep the second and third harmonics more than 50dB (electrical) below the fundamental for a 3mW peak-to-peak swing in its output.[2] However, this figure cannot be maintained if the temperature varies or as the device ages unless the rear facet is monitored.[3] The laser's high cost and increased current requirements make it unsuitable for the linear link project.

The light emitting diode (LED) is much less sensitive to temperature and aging induced changes. Despite these advantages the LED cannot easily be used as the source for analog transmission of data. The second harmonic dominates the harmonic distortion (H.D.) in a typical LED, limiting the H.D. to -35dB below the fundamental for 100mA p-p current swings which would be required for this project.[4] More importantly, it is not desirable to transmit D.C. signal levels due to the typical -0.3% $^{o}C^{-1}$ derating of power output[5] of a Burrus type device and the subsequent difficulty in maintaining 0.1% non-linearity through the received D.C. amplifier stages. There have been LED linearizing schemes demonstrated[6] but they do not overcome the D.C. amplification process and moreover complicate the autoranging scheme.

For these reasons, a strictly analog transmission scheme has been ruled out. Digital transmission offers the advantage that the source linearity is not critical: - all that is required is that the receiver be able to distinguish between two source drive conditions. Digital systems can be as accurate as desired, the trade-off being increased data conversion time. However, in addition to be decidedly more complex than analog systems, digital systems require precise synchronizing of the clock pulses at the remote and control units.

A more suitable alternative for low frequency applications, such as this link, is to use a voltage-to-frequency (V-F) converter. Inexpensive, high quality V-F and F-V integrated circuits are readily available. The V-F converter produces a continuous train of pulses of fixed duration (see Fig. 1). The period between these pulses is linearly proportional to the applied voltage. The receiver has only to detect the presence or absence of a pulse, similar to digital transmission, except that no sync pulse is required. The detected pulses are amplified and sent through a simple low pass filter to regain the original waveform. The demodulation technique is much simpler and less sensitive to pulse "jitter" at the receiver than are digital schemes.

In order to incorporate an autoranging capability three additional functions are required. First, a magnitude peak detector combined with a window detector is required to ensure that the gain setting is in its proper range. Secondly, a programmable gain amplifier must be designed that can maintain $\pm 0.1\%$ nonlinearity on all 6 gain stages covering two decades. Finally, some means has to be devised to allow the remote to unambiguously tell the control unit what gain level it is operating at.

Without resorting to a wavelength division multiplexed (WDM) system, it is difficult to simultaneously send two pieces of information down the fiber when one signal is in a pulse coded format. It turns out to be simpler to have the gain selection made at the control unit and to have the control send a signal back to the remote instructing it as to what gain is to be used. (See Fig. 2) Thus, the fiber carries a different signal in each direction: an information signal from the remote to the control and a gain selection signal from the control back to the remote. The bidirectional transmission of information allows for considerable flexibility of operation enabling deliberate manual override of the gain signal to the remote.

While the variable gain amplifier is of a conventional design, the gain selection process is more subtle. Autoranging systems usually have the luxury of sampling the input before the amplifying stages. Of necessity, the strategy of the linear link dictates that the gain selection be made after the signal has already been amplified. Thus, some method had to be devised to keep track of the previous history of the gain instruction. Circuits designed for this and the other stages will be discussed in a subsequent section.

DESCRIPTION OF OPTICAL COMPONENTS

Lower cost, reduced temperature sensitivity and simpler biasing schemes were the prime reasons for choosing LED's over lasers for the light source and PIN's over APD's for the detector. The characteristics of the LED, PIN and fiber used are listed in Figure 3.

The LED is a Burrus type[7] double heterostructure LED having its peak emission at 8300Å. The temperature dependence of the output power with temperature was measured to be -0.25% $^{\circ}C^{-1}$ (over the temperature range $0^{\circ}C$ - $50^{\circ}C$). This dependence results from a compromise with device thermal resistance in the choice of confining layer composition. Over the rated operating range ($0^{\circ}C$ to $50^{\circ}C$), the light output would vary less than $\pm 7\%$ about its room temperature value.

The LED, manufactured at Bell-Northern Research, had its active layer level doped p-type at a concentration of $10^{18} cm^{-3}$. This doping level results in the medium speed, highest radiance product of the three versions marketed by Bell-Northern Research.

The intrinsic rise time of these devices were 10nsecs (10%-90%) but in this application is limited by the slow risetime (120 nsec) of the current pulse. The radiant output was increased by $\sim$20% by chemically roughening the first confining layer surface. Use of a flat-ended fiber with an NA = .22 allows 150μW to be coupled in when 100mA is passed through the LED.

The PIN is an RCA 30808 photodiode. The dark current at $25^{\circ}C$ was $\sim$1 nA, rising to $\sim$1.5nA at $50^{\circ}C$. Under the system's biasing arrangement (-12V, 10kΩ load), its risetime was limited by the associated RC time constant. The observed photocurrent when the LED was modulated in circuit thus had a rise time ≈250 nsec.

The fiber was a graded index Ge coped sample fabricated at Bell-Northern Research. The core diameter (85 μm) was slightly larger than the LED emitting area to avoid coupling losses resulting from area mismatching. As the LED/fiber coupling efficiency is proportional to the fiber $(NA)^2$, a relatively large NA=.22 was used. The present trend for long distance links appears to be towards smaller NA's to minimize multimode dispersion but is immaterial for this application. The 3.8dB/km attenuation at 8300Å represents a high quality product specification available from several suppliers.

The feasibility of bidirectional data transmission in optical fibers is determined by the level of optical crosstalk falling in the pass band between the transmitter/receiver pair at the same station. All components and fiber joints must be carefully constructed to avoid spurious back-reflections which degrades the signal to noise ration (S/N) at the receiver. The optical coupler which combines the LED & PIN pigtails is the most critical component in a system of this type. Several ultra-high isolation couplers have been described[8] but their complexity and cost are not justified in a system that has the large noise margin this one has. Instead, a simpler fiber fusion technique was used to construct couplers possessing intrinsic isolations of approximately -50dB.

Referring to figure 4, the coupler is formed[9] by loosely twisting two fibers together and fusing them together using a gas torch. The flame is removed when the desired splitting ratio is achieved. A 2:1 or 3:1 splitting ratio was attempted. Larger ratios would have decreased the received optical power while smaller ratios would have resulted in an increase in the coupler's loss. The free end of the tap is not required and thus was broken off and potted in epoxy having approximately the same refractive index. The potting procedure increases the isolation from -20dB to -50dB, the latter limit being probably determined by the very slight index differences that still remain at this termination.

This observation demonstrates why conventional demountable one-to-one splices not employing anti-reflection coatings or immersion oils have to be avoided in a bidirectional system. In most envisioned applications, this unit would not be moved after installation so that permanent fusion splices were used to join the fibers.

This type of splice is formed simply by butting the two fibers together and fusing them together with a torch. Surface tension effects help to align the cores during the fusion, resulting in a splice having an insertion loss of only $\sim$.15dB and negligible back reflections. Both couplers and splices have been epoxied into styrene packages for mechanical protection.

The LED's launch light into the main ports while the PIN's receive light from the tap fiber. While theoretically the system S/N does not depend on which port the LED emits into, in practice the LED should not launch power into the system via the tap. This launching condition would excite proportionally more lossy, higher-order modes than injection through the less distorted main trunk waveguide. Additionally, the chemical roughening of the LED surface results in a back reflection which is lower than if the PIN had been on this pigtail. The importance of these reflections is demonstrated by the S/N calculation carried out in Appendix A and summarized in Fig. 5. The dominant source of optical crosstalk is seen to be reflection from the end faces at the opposite termination. This reflected light has to travel the length of the fiber and be attenuated twice whereas the signal only suffers the fiber attenuation once in reaching its intended PIN. Thus, due to this differential attenuation, the optical crosstalk improves with fiber length until it is ultimately limited by the coupler crosstalk (occurs when $L \approx 10$km) and Rayleigh backscattering.[10] Although Rayleigh backscattering does cause problems in some systems (primarily due to increased receiver noise and not due directly to intersymbol interference since the latter can be avoided with care)[10], in this link, the Rayleigh limit would never be approached.

An attempt was made to minimize the reflection at the fiber ends. An index matching fluid was used to occupy the space (~30 μm) between the cleaved fiber end and the solid state devices. Although this strataegm eliminated the 4% glass/air reflection, there was still some light coming back from the device surfaces. The isolation achieved for a 10m link was -17dB and was adequate for the link. Thus, polishing the fiber ends at a small angle was not required as it would be in systems requiring maximum isolation.

ELECTRICAL CIRCUIT DESCRIPTION

The linear link modulation scheme was built around the Intech A-8402 voltage-to-frequency-to-voltage converter. When configured in the V-F mode, (see figure 6) a capacitor C_{INT} is connected between the output and the inverting input of the internal op amp forming an integrator. The voltage applied to R_{IN} is summed by this circuit until the charge stored on the capacitor is sufficient to trigger a one shot (V(trigger)$\approx$ 0.7V). While the one shot is high, it turns on the output transistor and also activates a current source to discharge C_{INT} in preparation for the next integration cycle. After a time $T_{OS} = R_{EXT} \cdot C_{EXT}$, the monostable falls low, turning off the output transistor and current source, starting the integration cycle again. R_{EXT} was chosen to be a metal film type and C_{EXT} an NPO ceramic to minimize temperature dependances. The values of R_{EXT}, C_{EXT} were chosen to produce T_{OS} = 1.05 μsec, judged to be most appropriate for system performance.

A mylar type capacitor was used for C_{INT} in order to minimize gain errors resulting from charge leakage. The numerical value to C_{INT} is not critical so long as it is large enough to keep the current source from saturating the op amp and yet small enough to produce significant voltage variations. Resistor R_{OFFSET} supplies a constant current to the integrator. This current sets the minimum trigger rate of the one shot. With zero volts input, R_{OFFSET} was adjusted to produce an output pulse train of frequency 92 kHz. R_{IN} was adjusted to produce f_{OUT} = 415 kHz when the applied voltage was +10 Volts. All other voltages between 0 and +10V can be characterized by intermediate frequencies. The minimum pulse frequency was chosen to be well above the highest signal frequency ($\approx 20kH_z$). The upper limit was chosen to provide a large dynamic range without encountering any non-linear converter responses. As the output transistor can only sink 8 mA, it was used in turn to drive a second high speed transistor capable of the currents ($\approx$ 50 mA) required to drive the LED.

A slight re-arrangement of external connections is all that is required to have the same IC perform the inverse operation, (see figure 7). With no incoming pulse train, the internal op amp is configured in the usual inverting amplifier configuration, producing a DC voltage at the output dependant on the ratio R_{OFFSET}/R_{FB} .

A negative-going TTL-level pulse at pin 6 will trigger the one shot. As before, the one shot activates the current source for a period again given by $R'_{EXT} \cdot C'_{EXT}$. While the monostable is high, the current source pulls a constant current i out of the inverting output. This extra current can only come from the output of the op amp. Thus, while the current source is turned on, the output rises by $i \cdot R_{FB}$. R_{filter} and C_{filter} are just used to provide some filtering action prior to the main filter section.

Due to the action of the monostable, the shape of the incoming pulse has no effect on the output voltages appearing at pin 7 so long as the time during which the incoming pulses remain below 0.7V is less than $T'_{OS} = R'_{EXT} \cdot C'_{EXT}$. If the incoming pulse length is longer than T'_{OS}, the one shot will be triggered twice per pulse. It was desirable to make T'_{OS} as long as possible to achieve high resolution and still be less than the rep rate for the highest incoming frequency. T'_{OS} = 2.25 μsec was selected as it was reasonably close to the minimum repetition period = 2.45 μsec.

To be useful, this output must be strongly filtered to smooth out the high frequency output pulses and approximate a low frequency, continuous analog output. Ideally, one would like to have a filter possessing a unity passband from DC to the maximum signal frequency and completely blocking all higher frequencies (see figure 8). In practice, filters never have such sharp attenuation knees. For this project an active filter was found to be most suitable. Active filters generally use phase-shifted feedback to enhance the attenuation resulting from simple RC filtering. As well as attenuating the out-of-band frequencies, active filters can be made to amplify the pass band frequencies resulting in reasonable signal levels at the output. Moreover, DC shifts are easily accomplished making the system calibration relatively easy. The particular active filter chosen was a fourth order Butterworth. The Butterworth filter possesses one of the flattest pass band attenuation curves as well as a very steep response fall off above the cutoff frequency f_o. f_o was taken to be 20kHz in order to ensure that there would be very little residual ripple resulting from the lowest pulse frequency 92kHz. In practice, the filter employed attenuated the 92kHz by -47dBV. Since the filter attenuation increases by-24dBV/octave, all other pulse frequencies underwent even stronger attenuation.

A basic data link could be made using just the circuits described. However, in order to sample bipolar signals (the V-F is limited to 0 → +10V input potentials) or to increase signal resolution, an amplifier controlled by the receiver can be used to process the signal of interest to make it compatible with the V-F unit.

The control process starts by sampling the output of the active filter using a magnitude peak detector. This circuit is fast enough to track the magnitude of the positive and negative signal excursions. The absolute value of the peak voltage is held by an RC circuit possessing a 20 msec time constant (see figure 9). The voltage held by the capacitor is compared to the reference voltages on a window comparator. As the table in figure 9 shows, if the output voltage falls below 3.4V or above 8.5V it will trigger an "increase gain" or "decrease gain" signal respectively.

In order to understand how this signal works, it is necessary to refer again to figure 9. There is an array of eight comparators fed by the output of summing amplifier A_1. Any comparator which is high will turn on the LED connected to its output. The current through the LED is limited to 15 mA by 500 ohm variable resistors in series with it. The wiper on each resistor is set so that when the comparator is high and current passes through it, the voltage at the wiper is just sufficient to keep its comparator high. A diode array serves to pick the highest voltage (generated by the highest comparator held high) and feeds it back via A_1 to the input. Thus, this feedback ensures that once a certain pattern of comparators are high, they will remain set. The "increase' and "decrease" gain commands take the form of voltage transients summed at A_1. As illustrated, these commands are decaying voltage transients but since the comparator feedback is through a capacitor also, the output of A_1 is approximately a voltage step. The height of this step is just sufficient to switch one comparator at a time.

It is important to note that the gain level comparators will switch very fast, instructing the remote unit to change gains in ~2msec. Subsequent output voltages having the new amplification have the remaining 18msec to ensure that the output of the peak detector falls within the normal window comparator limits. If, at the end of this time, the output is still out of range, the gain will be incremented again.

With the feedback system used, there is no chance that the actual gain level is different from the indicated one unless there is a serious circuit fault. This possible ambiguity can be removed by manually over-riding the autorange circuit and addressing the gain levels sequentially. This back-up provision could be important in many situations and could not be implemented at all if the gain selection had been made at the remote.

The voltage from the diode array used in the feedback, is fed also to a second V-F converter. The remote unit decodes this pulse train by a simple RC filter (as opposed to a second F-V since linearity requirements are relaxed), to become the gain control signal for the remote amplifier.

The remote amplifier (see figure 12) is composed of a pair of dual op amps selected for high input impedences and large output voltage swings. The high input impedence ($\sim 10^8\Omega$) of the voltage follower input stage minimizes source loading while the op amp's internal circuit connections allow its output to be driven to within 0.7V of either supply rail. This capability is possessed by few op amps and its absence would be the dominant non-linearity at high signal levels.

With a control signal corresponding to x0.5 (or in the absence of any control signal) all the resistors in the array are connected in parallel resulting in an equivalent resistance of 5kΩ. When the control signal increases to change the state of the first comparator, it shuts the assoicated FET switch, causing the equivalent resistance to increase to 10kΩ(and hence the gain from x0.5 to x1.0). After amplification the voltage level is shifted by 5V (derived from a precision voltage source) to be compatable with the V-F input range. The resistors used in the gain selection are all 1% metal film to reduce temperature effects.

SYSTEM PERFORMANCE

For link lengths up to 1 km, 50 mA current pulses were driven through the LED, although the amplitude of the pulse could be set arbitrarily by suitable selection of a series resistor (see figure 6). The V-F controlled driver produced square current pulses possessing rise and fall times less than 150 nsec. The receiver was relatively insensitive to the photo-generated pulse shape due to the presence of the monostable in the F-V converter. This condition allowed considerable flexibility in the design of the receiver front end.

A single stage, +60dBV amplifier/pulse conditioner was formed by a high speed comparator to trigger the F-V (see figure 13). The switching speed of the comparator was determined by the amount of voltage overdrive applied to its inputs. The inverting input monitored the photovoltage generated across a 10 kΩ load. While the rise-time of the photovoltage was $\sim$1 μsec, its 30mV amplitude, coupled with 2mV of hysteresis resulted in an ideal trigger pulse having rise and fall times less than 100 nsec being applied to the F-V unit. Proper choice of decision level at the non-inverting input ensured that there was no change in the output of the F-V for $\pm$ 30% amplitude fluctuations in the received photovoltage. The pulses at relevant points in the circuit can be seen in figure 13. The net result was that each 1 μsec current pulse through the LED produced a 8.8V voltage pulse of half width 2.25 μsec at the output of the F-V unit. Filtering due to the capacitor connected to the inverting input of the F-V op amp can be seen to have increased the transition times of the pulse. It was this pulse which had to be subsequently filtered to obtain an output voltage with little residual ripple.

The table in figure 20 summarizes the measured system response. As there may be situations in which input signal conditioning would not be required, data was presented for systems both with and without the remote amplifier. The D.C. linearity was measured using high resolution ($\pm$ 1mV) voltmeters to measure input and output voltages as shown in figure 14. The best fit to a straight line was determined from twenty-one equally spaced data points covering the complete voltage range of the V-F. The measured deviation from this best fit for the V-F unit alone, (plotted in figure 14) was seen to be 5mV (0.03% of full scale). The errors inherent in the measurement were approximately $\pm$ 1.5mV so that the only significant departure from linearity occurred at the upper end of the voltage range. The same procedure applied to the output frequency of the V-F showed no corresponding deviation from a best fit in this region, indicating that the dominant source of non-linearity in the system was in the F-V section. At the higher voltages, the F-V was operating at 93% duty cycle which may have caused some heating induced changes.

The voltmeters used in the measurement had one second count periods so they were not affected by the small amount of noise present in the output signal. A large bandwidth instrument monitoring the output voltage would detect the high frequency pulses which still were passed, albeit strongly attenuated, by the active filter. The high frequency noise due to the lowest pulse frequency (92kHz) was 7 mV_{rms} and dropped rapidly at higher frequencies to a limiting value of $\lesssim$2 mV_{rms} as the

Butterworth filter caused even greater attenuation, (see figure 15. a $\rightarrow$ c). This high frequency noise was not considered troublesome since it was oscillatory and hence averaged to zero very quickly when measured on instruments having bandwidths comparable to the linear link bandwidth.

The residual noise in the system was measured with an RMS voltmeter having a measurement bandwidth of 30 kHz. The measured output noise voltage (at $V_{out} = 0\ V_{D.C.}$) was observed (see figure 16) to be independant of the amplifier gain setting. This result demonstrates that the remote amplifier itself possesses an intrinsically low noise contribution. The total system noise is thus dominated (see figure 15(d)) by uncertainties in the V-F-V conversion process. This uncertainty is strongly influenced by the power supply and internal reference stability. Thus in order to achieve these low noise figures, good supply isolation of the F-V and V-F from other circuits had to be employed as well as increasing the value of the capacitor on pin 13 of the A-8402.

One of the most accurate methods of determining the dynamic linearity of a four port network is to measure the harmonic content of the input and output voltages. Any non-linearity in the network transfer characteristics will result in the generation of higher order harmonics of the input voltage.

The total harmonic distortion (THD) of the V-F unit itself was low at all frequencies of interest. The primary source of system distortion was the amplifier at the remote station. THD was measured under all cases when the output swing was 8 V_{p-p} as would be typical when autoranging. THD(measured as diagrammed in figure 16) was observed to increase as the gain or signal frequency was increased. This effect is a fundamental limitation imposed by the operational amplifiers used in the various gain stages. Any operational amplifier, with their large open loop gains (typically 10^5 at D.C.) is intrinsically highly non-linear. This is useful if the device is to be used as a comparator, as for example in the detector circuit. For use as a linear amplifier negative feedback of the output signal applied to the input is commonly employed to reduce the distortion so introduced and still provide reasonable gain. A simple model was used to qualitatively explain the observed data, (see figure 17). The equivalent circuit analysis shows that if the signal gain is G (determined by R_f/R_{in}), the generated distorted signal (V_d) is attenuated by a factor $D = \left[(A_o(f)/G) - 1\right]^{-1}$ where $A_o(f) \equiv$ open loop gain of amplifier at the frequency (f) of interest. Since A(f) is required to fall off steeply in order to ensure amplifier stability, V_d becomes less attenuated and hence, relative to the signal, much larger. The table in figure 17 shows the same trends as figure 16 although an exact equivalence between the two is not implied. It should be noted that the THD was measured on an instrument possessing a bandwidth of several MHz so that the THD measured wholly in the system bandwidth is actually much less.

Nonetheless, the measured THD is extremely low, as the photo in figure 16 demonstrates. For comparison purposes, quality stereo amplifiers rarely achieve better than 0.5% THD at rated output and then over only a limited frequency range.

In any transmission system that employs a signal sampling scheme for encoding, the theoretical maximum frequency which can be transmitted is sampled twice per cycle by the system.[12] The sampling rate in the linear link varies with applied voltage from 92 kHz to 490 kHz as determined by the integration period of the V-F. The -3dB frequency of the link was set to be approximately 17 kHz. Thus, while it is being operated slightly below half of the maximum obtainable information rate the extra margin allows for much better noise performance.

The frequency response of the Butterworth filter and the total sytem response is shown in figure 18. The filter clearly determines the overall system frequency response as it should since all other circuits employed are much faster.

The system pulse response is also shown in the same figure. The response rise time to a step impulse is 18 μsec (10%-90%), with only a $<$ 8% overshoot and a setting time to within 1% of final voltage $<$ 50 μsec. The key to this fast response is the rapidity with which the chosen V-F module can follow these changes. The accompanying photo showing the output of the V-F when driven by a step pulse demonstrates that the A-8402 does indeed settle to its final frequency within 2 output pulses as it is specified to.

The remote amplifier gain is determined solely by the values of the feedback resistors used. The tightest toleranced resistors readily available in metal film (used because of their low temperature coefficient) is 1%, the actual gains could vary from their nominal values by 2%. In fact, as figure 16 showed, the gains are considerably closer to their nominal value particularly for the small gains when the percentage errors cancel out. It would be relatively easy (although expensive and time consuming on a production basis) to trim the resistors to achieve any desired precision. Gain values not withstanding, the D.C. system linearity on all gain settings is better than 0.1%. This performance could only be achieved by the use of J-FET's designed for electronic switch applications. Reed switches consumed too much current for the remote station when activated and CMOS switches not only have to be protected from negative voltage excursions, but are leaky at the voltage extremes and introduce excess non-linearities. The control voltage to the FET gate had to be held as close to the supply rail as possible when in the off state necessitating the use of MC 4558 IC's to effect the control. The "on" resistance is about 30Ω(negligible compared to 10 kΩ series resistor) and an equivalent "off" resistance of approximately 100MΩ.

The D.C. linearity and THD measurements on all gain settings were facilitated by manually setting the gain at the control unit. At any gain setting the "MAN/AUTO" toggle switch on the control can enable the autoranging option, (the green LED comes on when the toggle is in the "auto" position). The autorange will attempt to keep the absolute value of V_{out} between 3.4 and 8.0 Volts. Figure 19 (a) shows,for a symmetrical sine wave, that the peak detector will track both positive and negative encursions and moreover, can be seen to accurately find the peak value. The droop between the peaks is necessary to ensure that the peak detector will cause a gain change in a fixed time interval if the output level decreases. With the present selection of R and C used in figure 10, the decay time is approximately (1/50 Hz) in order to cover just the audio regime. This period can be easily adjusted but at the expense of the autoranging response time.

The actual gain switching is achieved very quickly (as figure 19 (b) shows despite triggering difficulties) and is essentially changed at the slew rate limit of the op amp. Note the absence of momentary transients during switching, indicating no oscillatory comparator behaviour. The autoranging control appears stable (except, as indicated, for certain voltages having a period $<$ 50 Hz) and reproducible. It allows only $\sim$4 msec of overload under extreme conditions and the gain has never been observed to be different from that indicated by the LED front panel.

The set-up procedure can be facilitated or the system checked by manually selecting "V ref" on the front panel. This isolates the variable gain amplifier entirely from the level shifter so that the V-F unit transmits the +5.000 V offset voltage.

CONCLUSION

A unique, versatile optical link has been designed and assembled using readily available components. The linear link's system performance is summarized in figure 20. The design objectives of high linearity, moderate bandwidth, low power consumption and variable manual/autoranging gain control have been met,thus qualifying the system for use in high accuracy monitoring situations. Additionally, a multiplexing capability has been demonstrated further extending the potential usefulness of the link. Due to the system's use of common parts and a single fiber to effect two-way information transfer, it is believed that the linear link as described herein could be economically produced and used to extend the viability of fiber optics to include industrial applications.

REFERENCES

1. Kato, D. "High Quality Broad-Band Optical Communication by Time-Division Multiplexed Pulse Analog Modulation: Non-linearity in Diode Lasers" Journal of Quantum Electronics, QE-14, May 1978, p.343.

2. Goodwin, A.R. et. al., "Narrow Stripe Semiconductor Laser for Improved Performance of Optical Communication Systems" Proceedings of the 5th European Conference on Optical Communications, 1979, p.4.3-1.

3. Kressel, H. and Butler, J., Semiconductor Lasers and Heterojunction LED's , Academic Press, New York, 1977, p.477.

4. Lee, T.P., "The Nonlinearity of Double Heterostructure LED's for Optical Communications", Proceedings IEEE, 1978, 65, p. 1408.

5. Springthorpe, A.J., private communication.

6. Straus, J., "Linearized Transmitters for Analog Fiber Links" Laser Focus, 1978, p.54.

7. King, F.D. et al., "High Radiance Long-Lived LED's for Analog Signalling", Proceedings IEEE, 123, 1976, p. 619.

8. Wells, W.H., "Cross-talk in a Bi-Directional Optical Fiber" Fiber and Intergrated Optics, 1, #3, 1978, p.243.

9. Special thanks to G. Duck for aid in coupler fabrication.

10. Straus, J. "Measurements of Frequency Dependance of Rayleigh Backscattering in Bidirectional Optical Systems" Electronics Letters, May 1979, p. 306.

11. Brophy, J. Basic Electronics for Scientists, McGraw-Hill, 1972.

12. Gagliardi, R.M. Introduction to Communications Engineering, John Wiley and Sons, Toronto, 1978, p.230.

Figure 1: Principal of Voltage-to Frequency (V-F) Conversion and Frequency-to-Voltage (F-V) Decoding

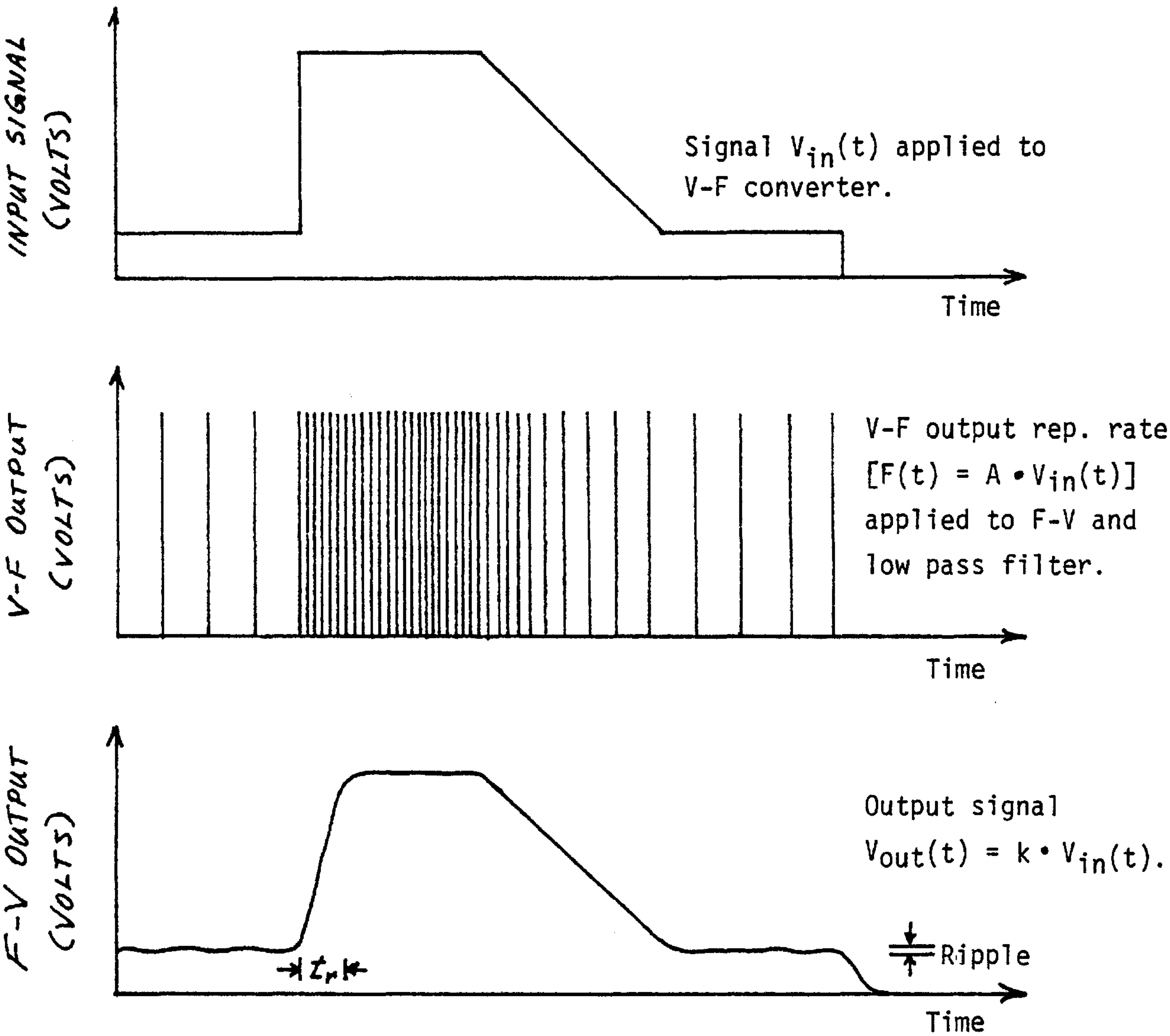

Frequency Allocation in System

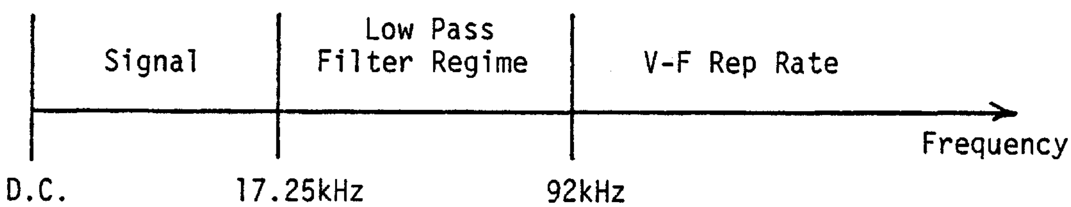

Fig. 2 - System Functional Diagram

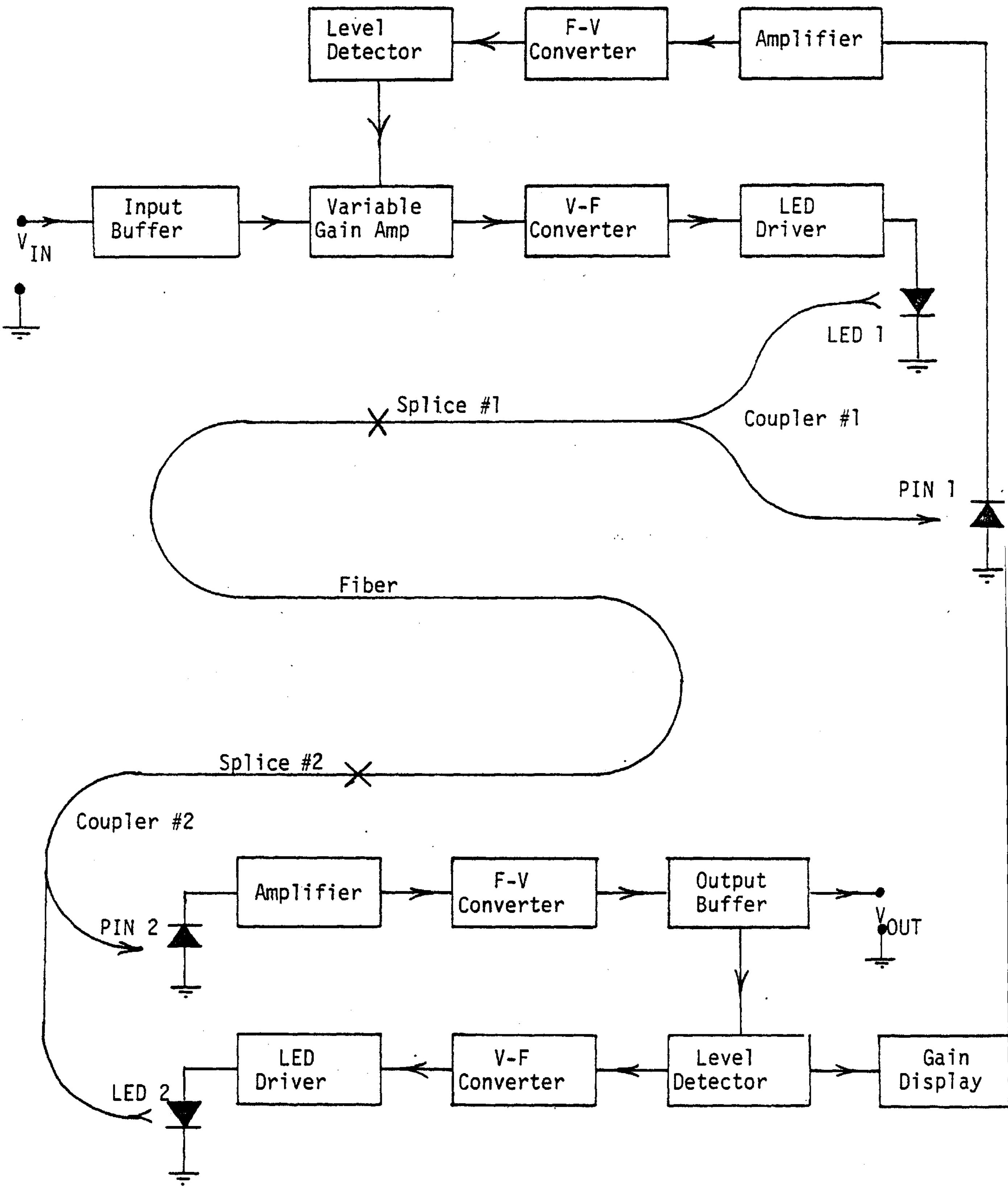

Figure 3 Optical Components

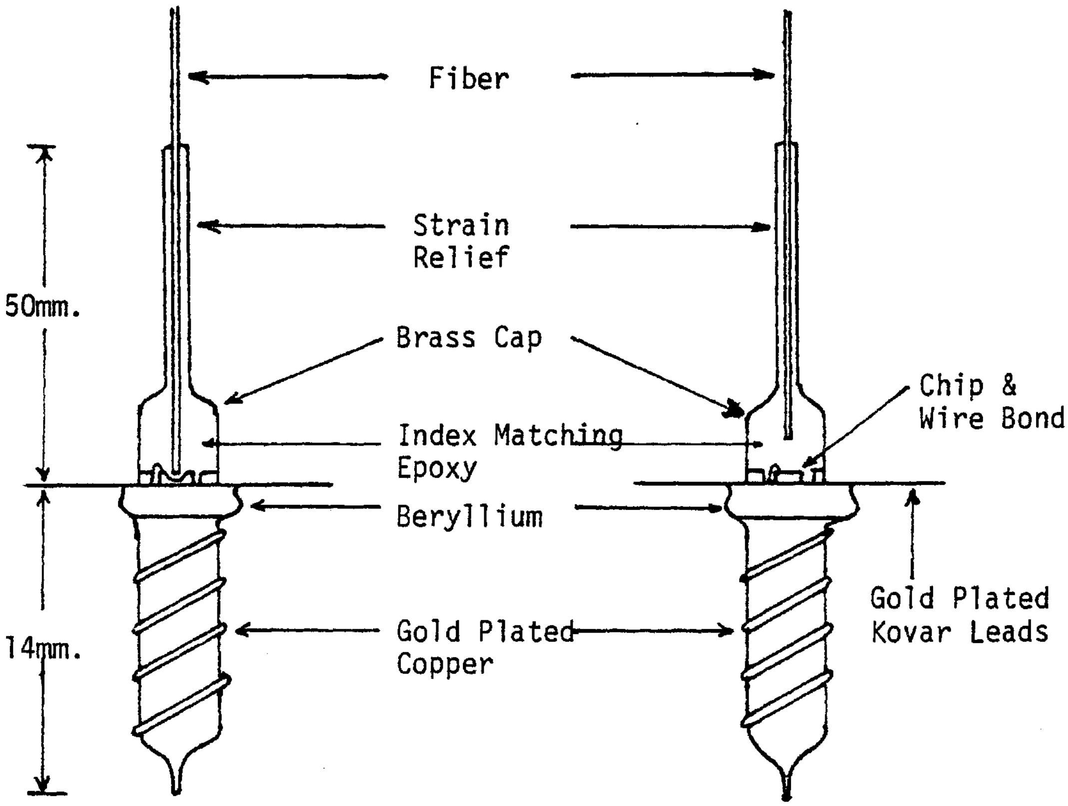

LED

λ = 8400 Å
$\Delta\lambda$ = 400 Å
τ(rise) = 10 nsec
Coupled Power= 1.5 mW/A

PIN

Responsivitity=0.5A/W
I(Dark) = 10nA
V(Breakdown) = 100V

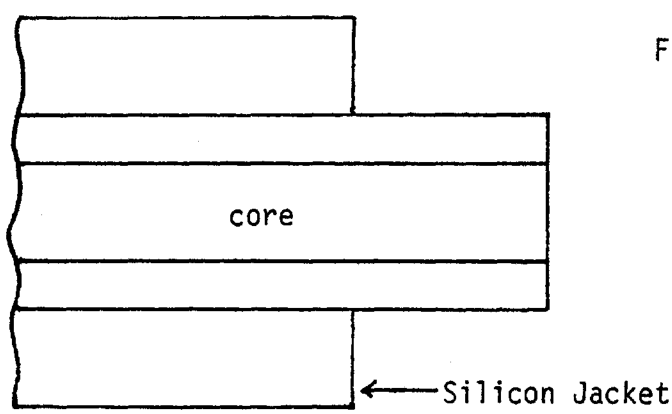

Fiber: Graded Index
NA = 0.22
α = -3.8dB/km

core = 85μm
O.D. = 145μm

Figure 4: Low Crosstalk Optical Couplers

Splitting Ratio = $L_1 : L_2$	(Typical: 3:1)
Coupler Loss = $10 \log([L_1 + L_2]/L_0)$	(Typical: -1dB)
Crosstalk = $10 \log (L_4/L_0)$	(Typical: -46dB)

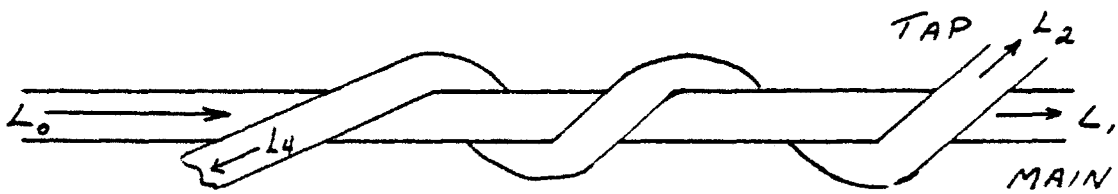

Free end potted in index-matching epoxy.

Couplers formed by cleaning fibers in chromic acid, loosely twisting them together and fusing them together with heat.

Figure 5: Crosstalk Calculation Summary

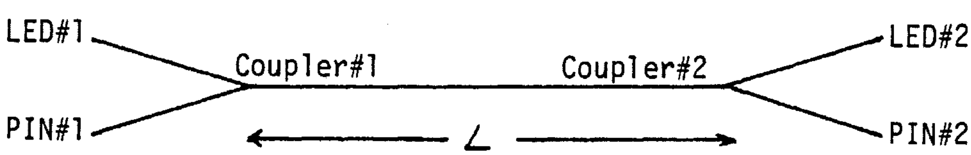

Signal Attenuation

LED#1 to PIN#2	$(-9.8 - (\alpha \cdot L))$
LED#2 to PIN#1	$(-11.1 - (\alpha \cdot L))$

Crosstalk

LED#1 to PIN#1	$(-28.8 - 2(\alpha \cdot L))$dB
LED#2 to PIN#2	$(-28 - 2(\alpha \cdot L))$dB

Signal/Crosstalk		Measured
At PIN#1	$(17.7 + \alpha \cdot L)$dB	15.5dB
At PIN#2	$(18.2 + \alpha \cdot L)$dB	19.5dB

Figure 6: Intech A-8402 Voltage to Frequency Converter

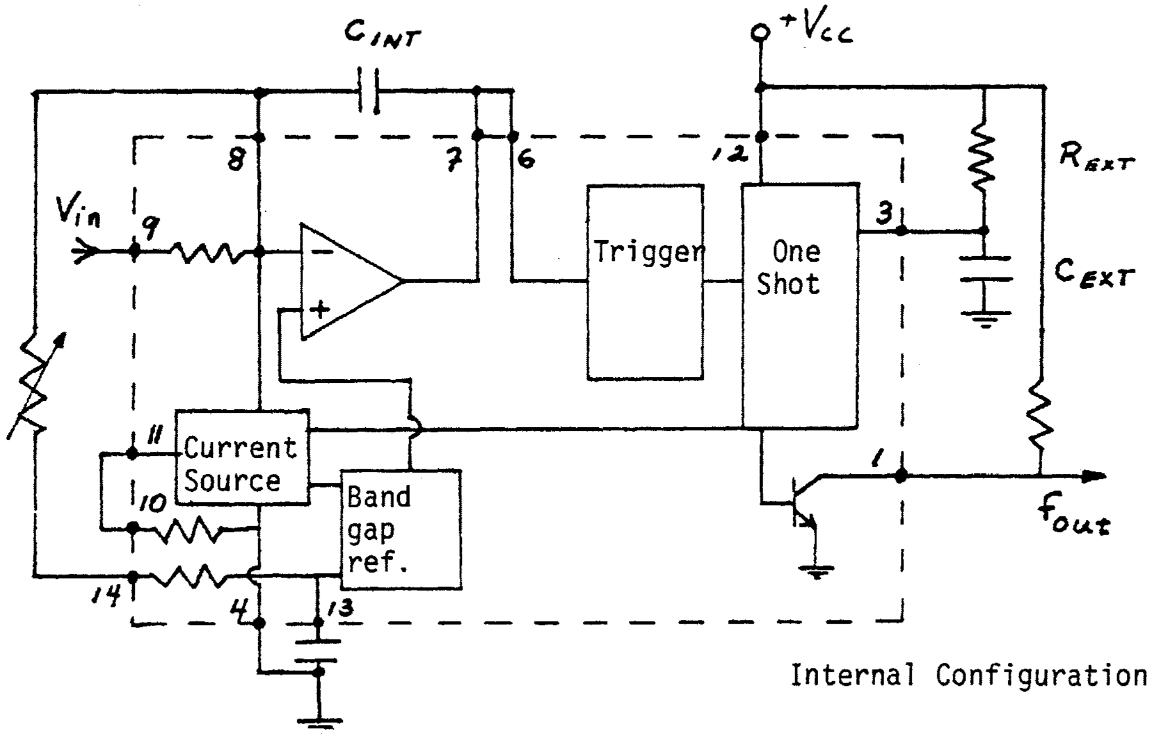

Internal Configuration

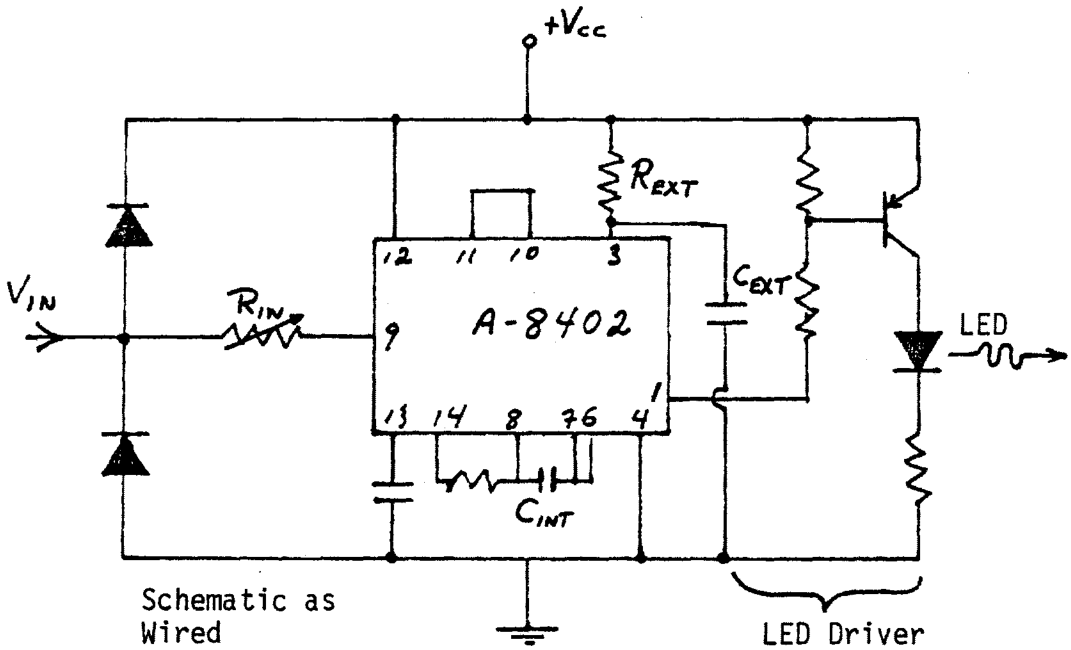

Schematic as Wired

LED Driver

Figure 7: Intech A-8402 Frequency to Voltage Converter

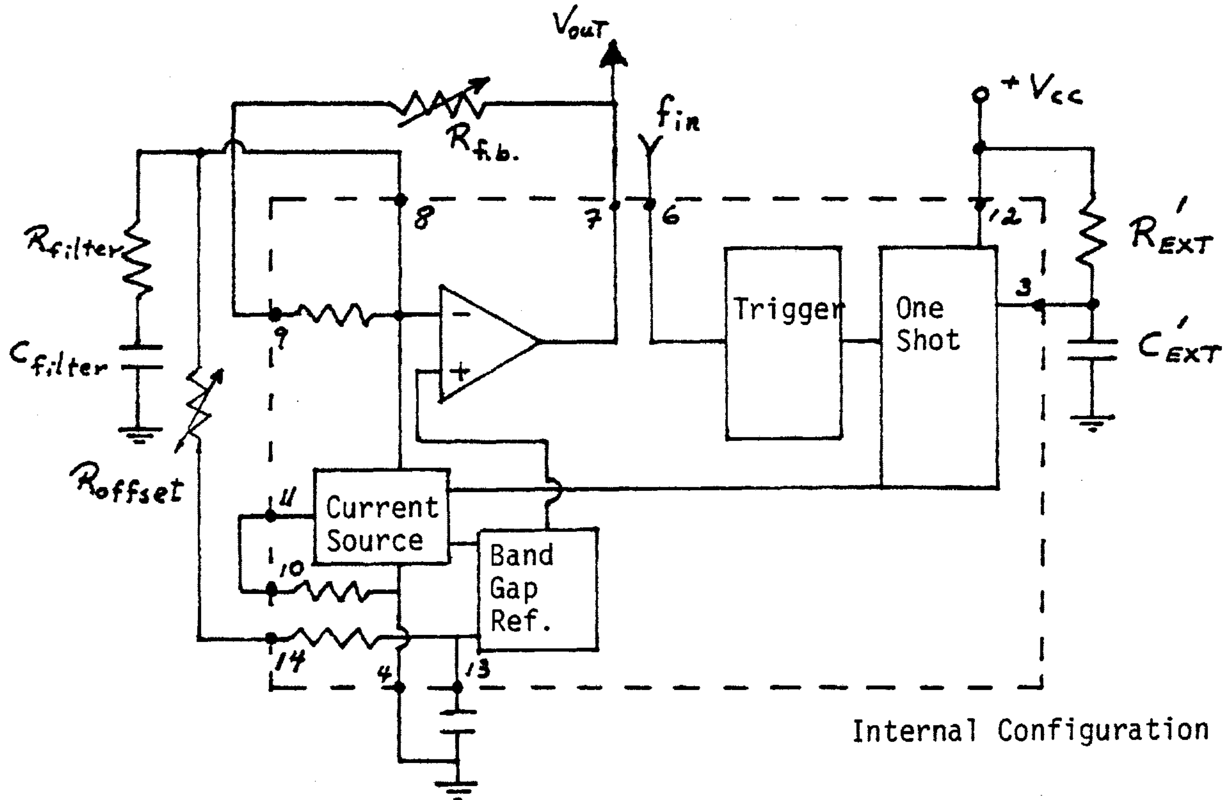

Internal Configuration

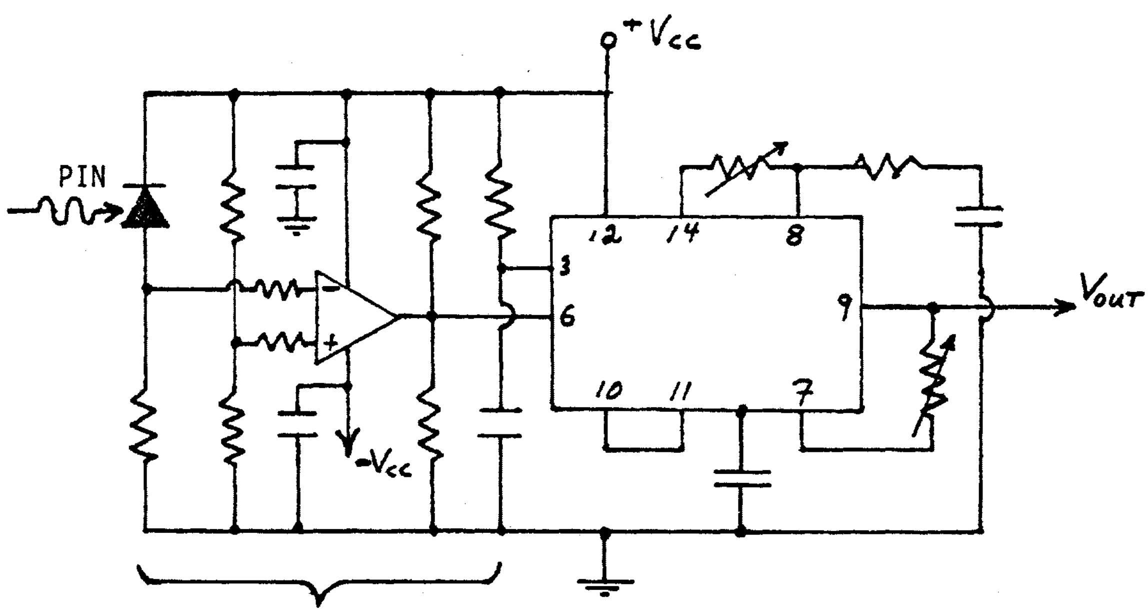

Detector Circuit

Schematic as Wired

Figure 8: Active Low Pass Filter

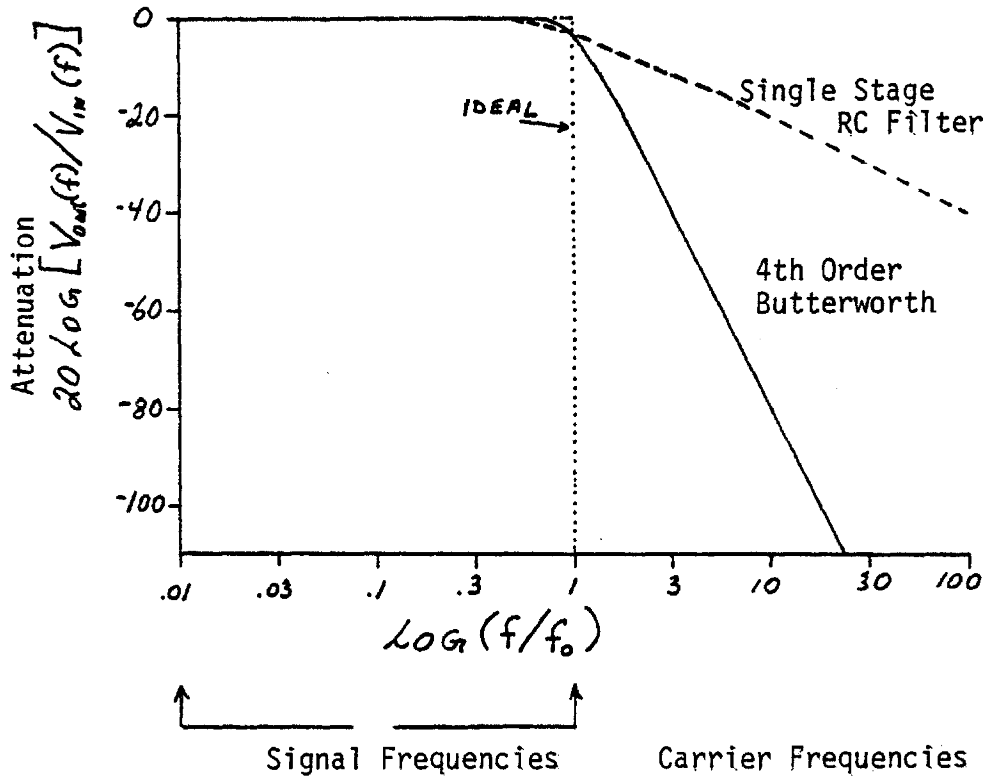

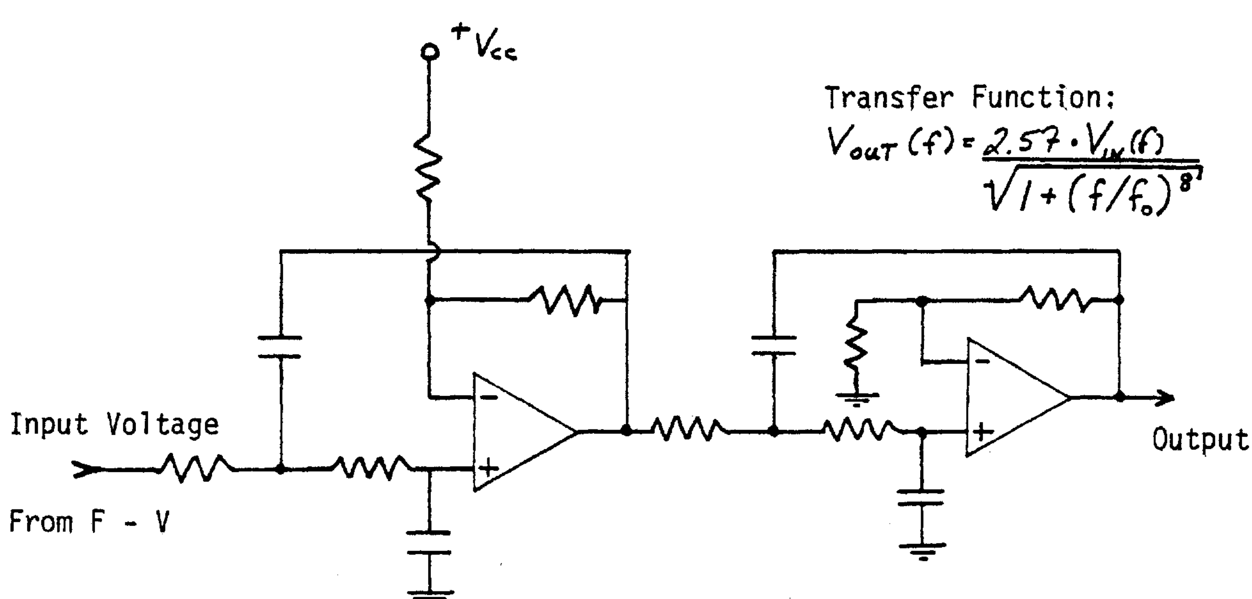

Figure 9: Gain Control

Information Flow

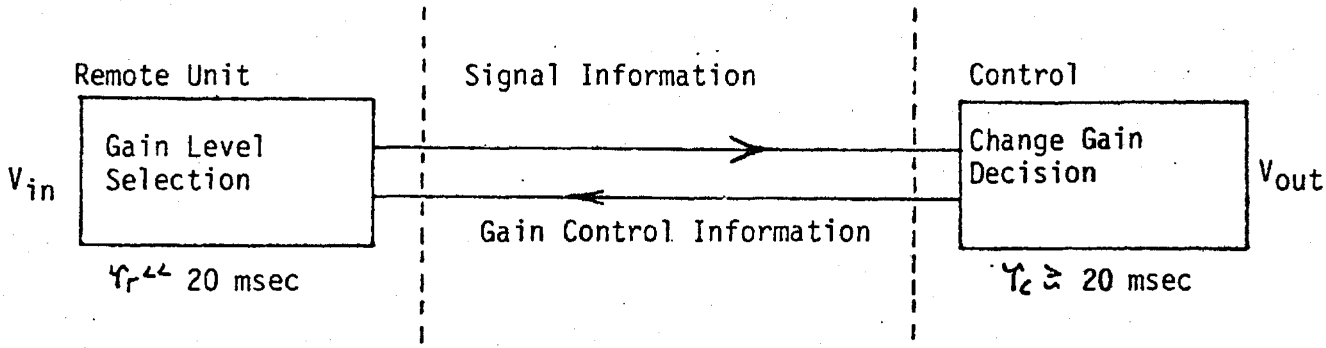

Gain Control Signal Synthesis

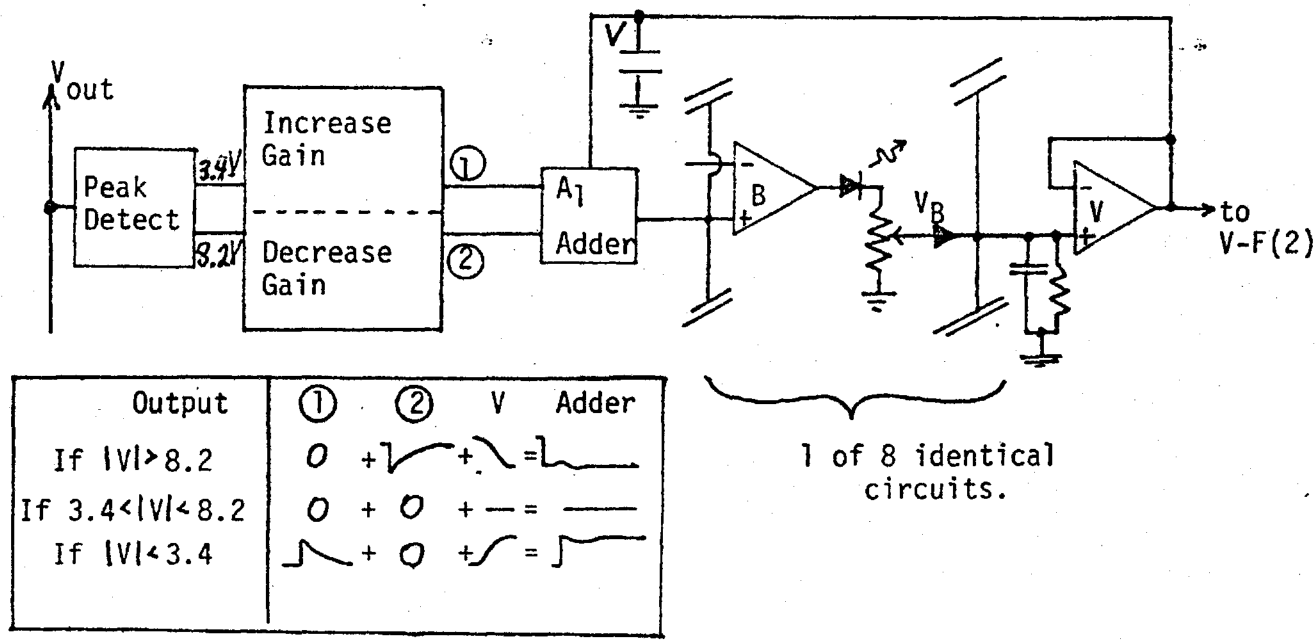

Voltage Gain	Input Voltage Range	Output Voltage Range	F
x0.5	5V < |V| < 10V	2.5 < |V| < 5.0	0 or 573Hz
x1.0	2.5 < |V| < 5.0	2.5 < |V| < 5.0	1.110kHz
x2.0	1.0 < |V| < 2.5	2.0 < |V| < 5.0	1.572kHz
x5.0	0.5 < |V| < 1.0	2.5 < |V| < 5.0	1.966kHz
x10.0	0.25 < |V| < 0.5	2.5 < |V| < 5.0	2.429kHz
x20.0	0.1 < |V| < 0.25	2.0 < |V| < 5.0	2.850kHz
x50.0	0 < |V| < 0.1	0 < |V| < 5.0	3.287kHz

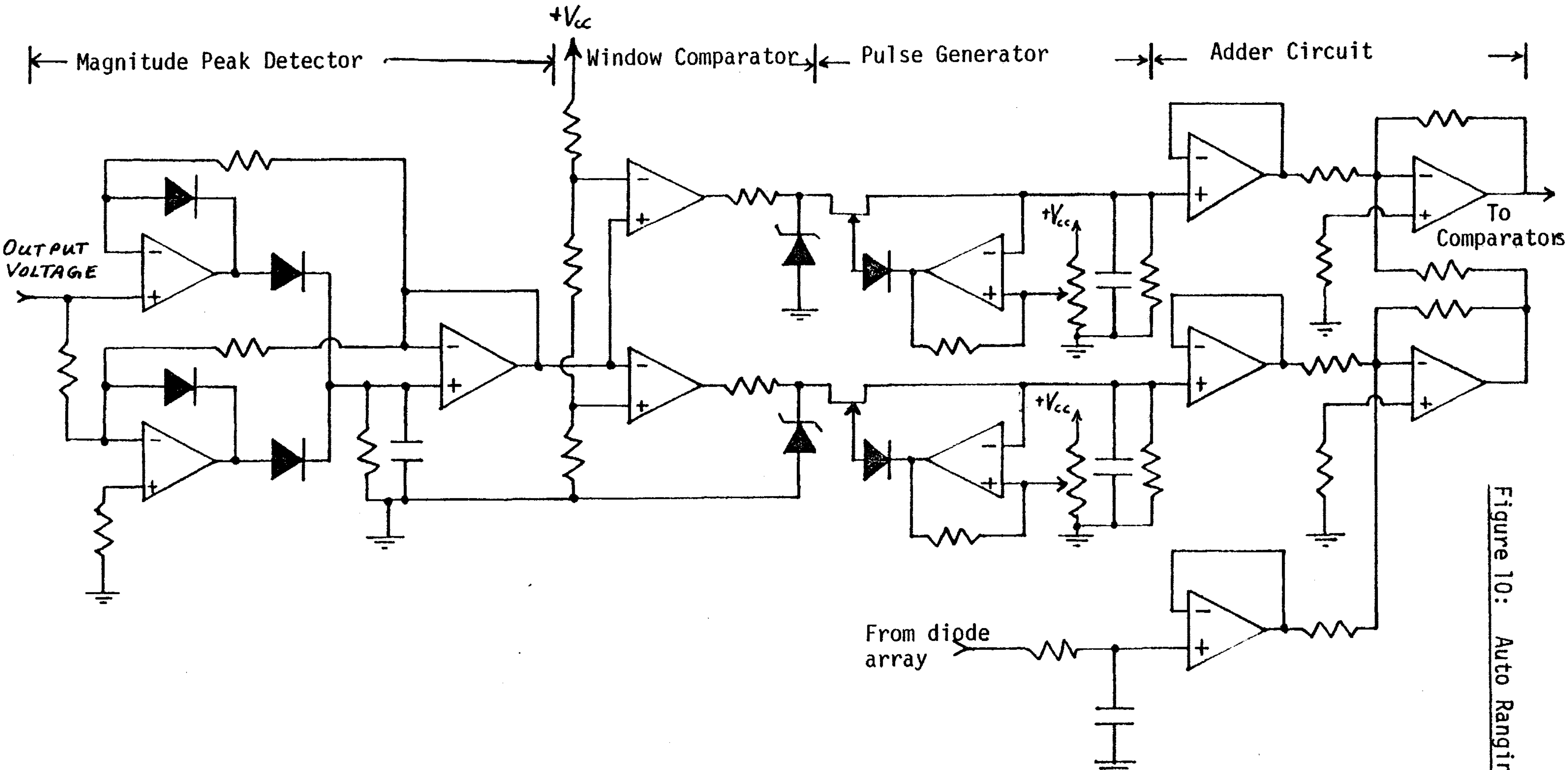

Figure 10: Auto Ranging Schematic

Figure 11: Schematic of Gain Control Signal Generating Circuit

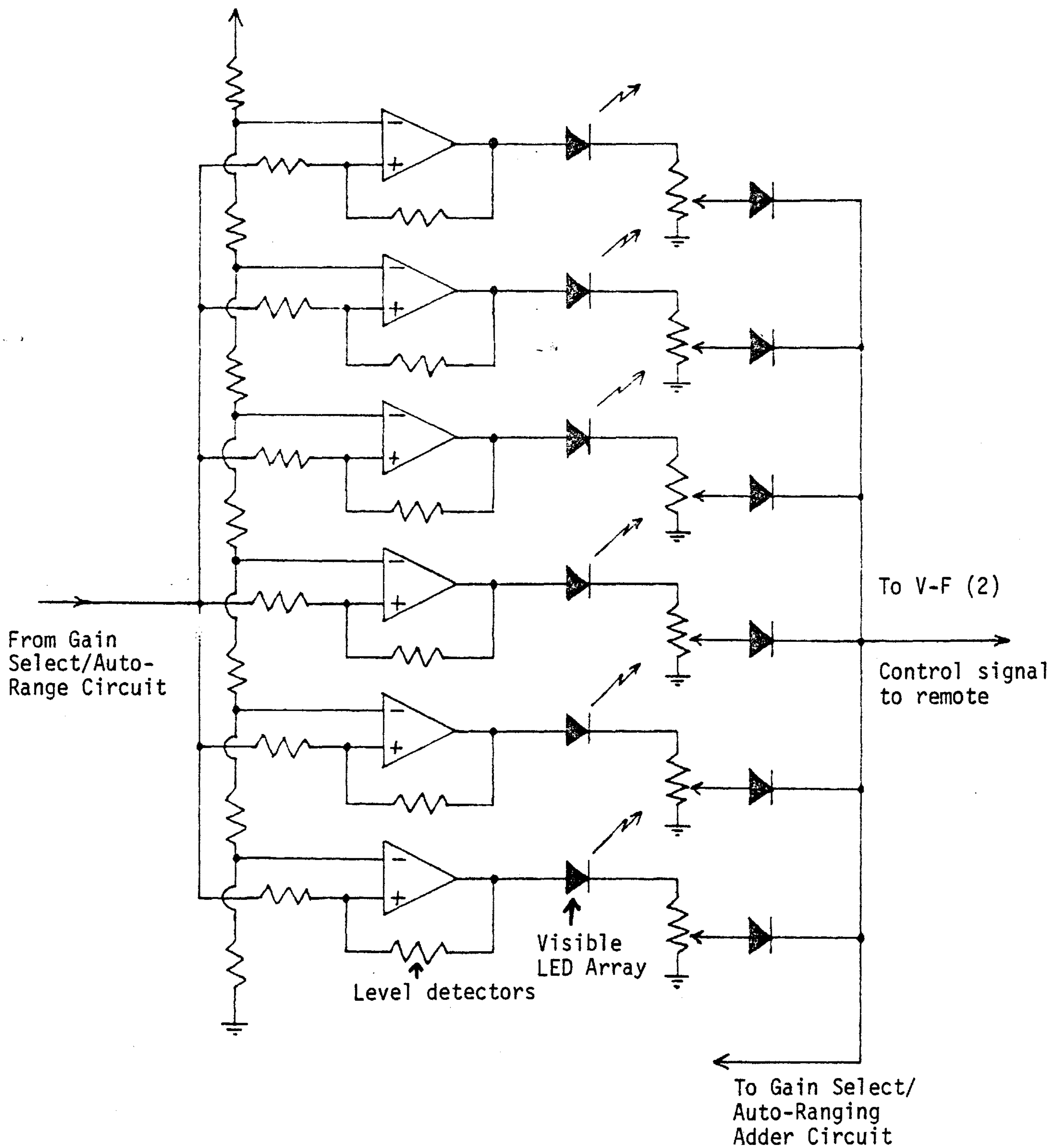

Figure 12: Remote Amplifier Schematic

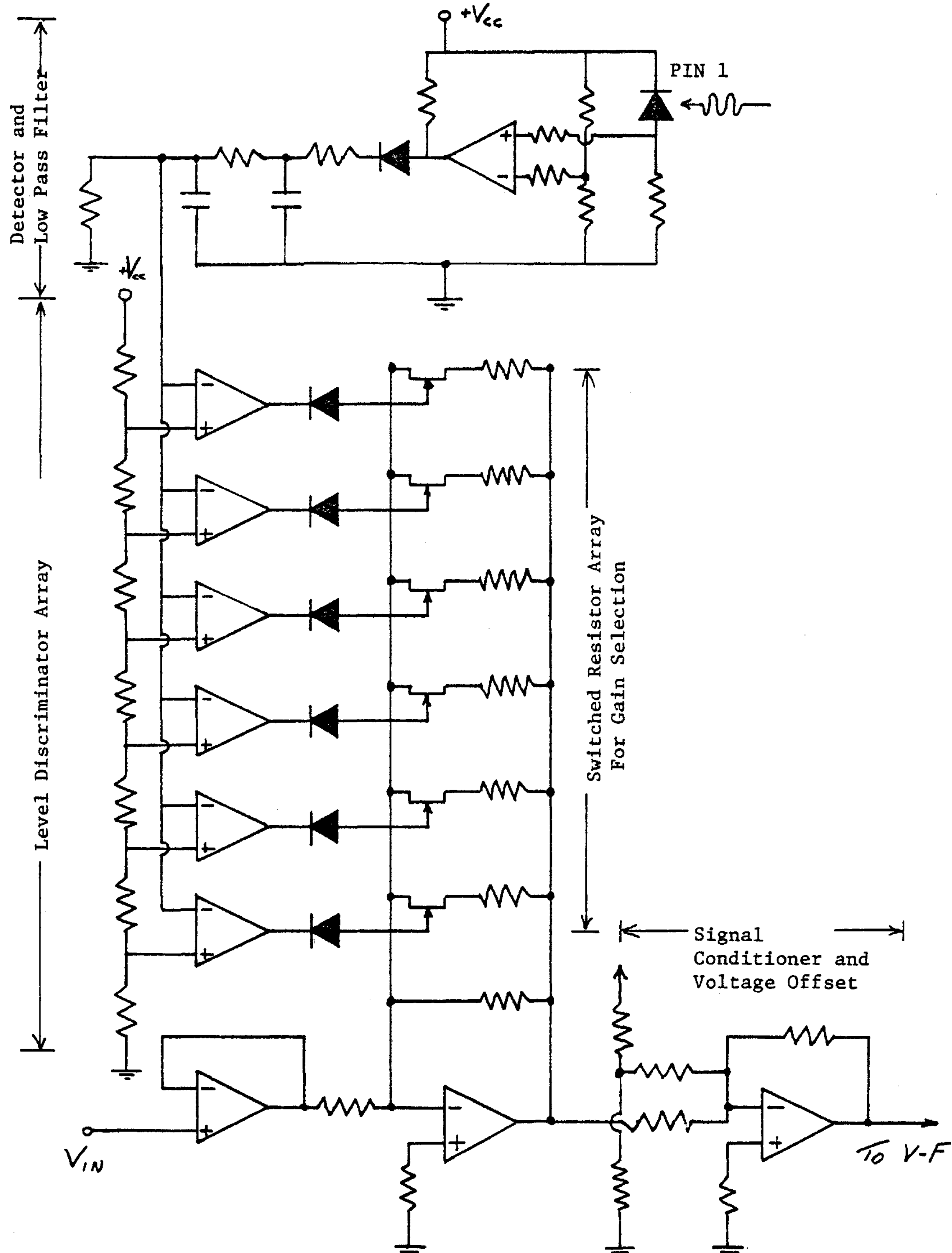

Figure 13: Voltage Waveforms at Selected Points in System

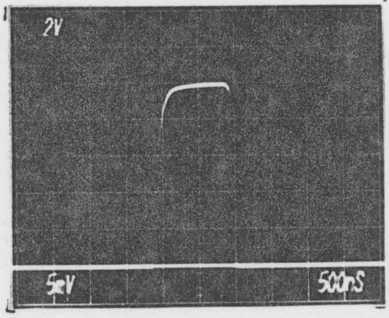

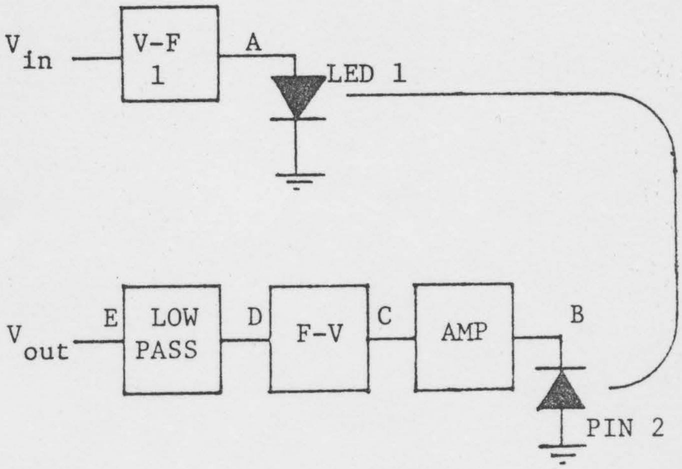

A. Current Pulse to LED (20mA/DIV) Light output would appear identical

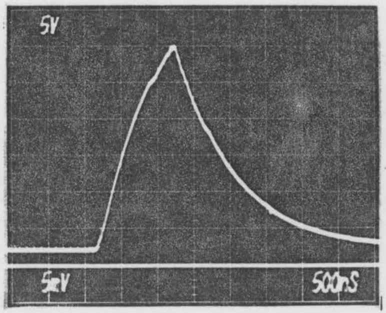

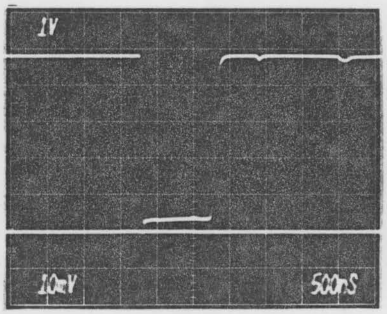

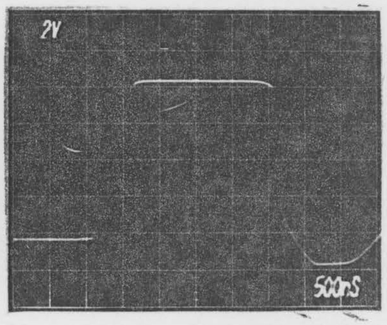

B. Output of PIN viewed across Load Resistor (RC rise time limited)

C. Output of Amplifier/ Pulse Shaper. Voltage has been inverted to be compatible with F-V

D. Output of F-V

E. Sample Wave Forms

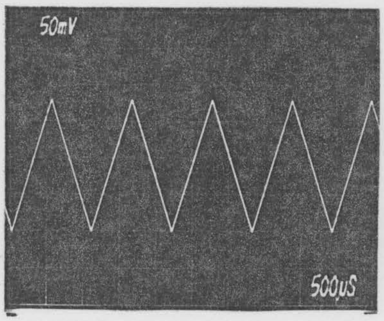

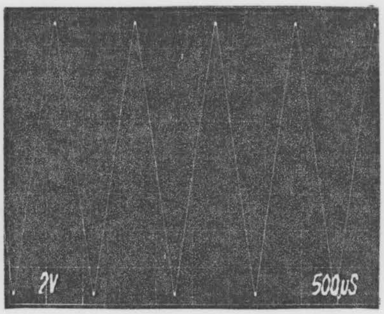

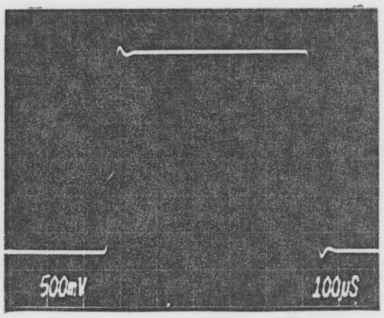

V_{in} = 1kHz sine wave

V_{out} replicates V_{in} accurately

V_{out} when V_{in} is a voltage pulse.

<u>Figure 14: V-F-V D.C. Linearity</u>

Deviation from linearity for V-F process

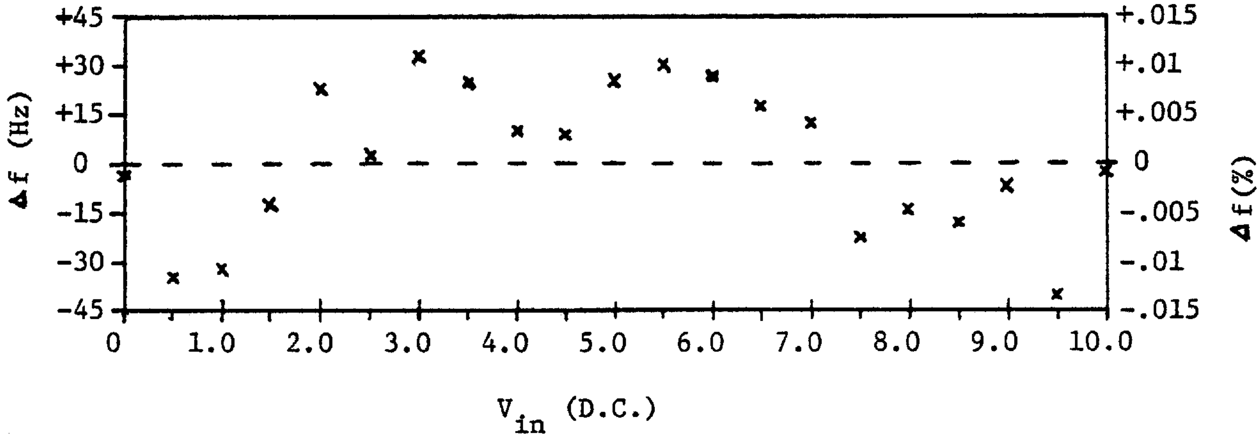

$\Delta f \equiv$ (measured frequency) − (frequency calculated from best fit to a straight line)

$\Delta f\% \equiv \Delta f/(f_{max} - f_{min})$

Best fit: $F_{out} = 32.276 \text{ kHz} \cdot V_{in} + 92.429 \text{ kHz}$

Deviation from linearity for V-F-V process

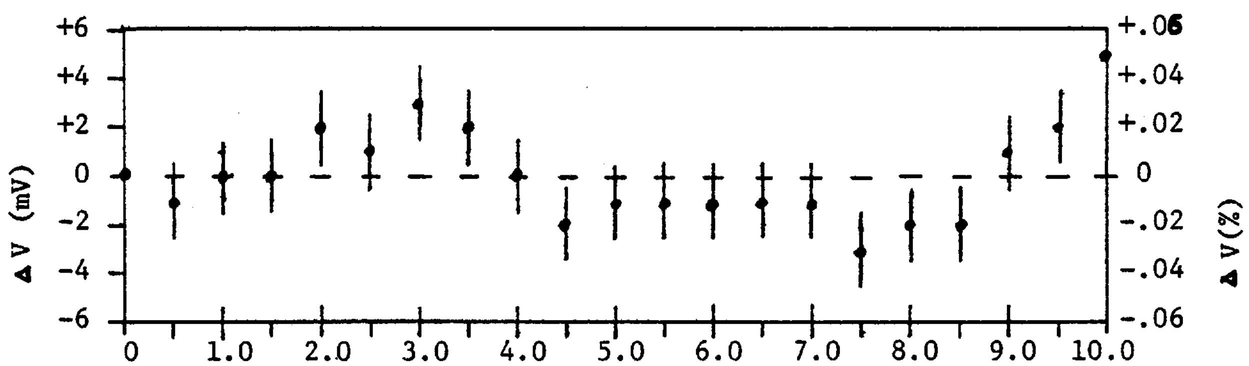

$\Delta V \equiv$ (measured V_{out}) − (V_{out} calculated from best fit of data to a straight line)

$\Delta V\% \equiv \Delta V/(V_{max} - V_{min})$

Best fit: $V_{out} = 1.680 \cdot V_{in} - 8.404 \text{ V}$

Figure 15: Noise in System Output

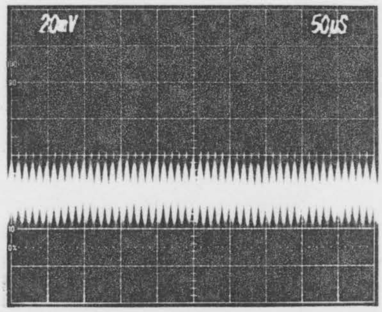

a) $V_{in}(V\text{-}F)=0.0V_{D.C.}$

$V_{out} = -8.7V_{D.C.}$

$f = 92$ kHz

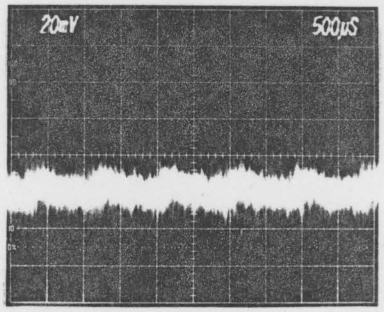

b) $V_{in}(V\text{-}F)=+5.0\ V_{D.C.}$

$V_{out} = 0\ V_{D.C.}$

$f = 253$ kHz

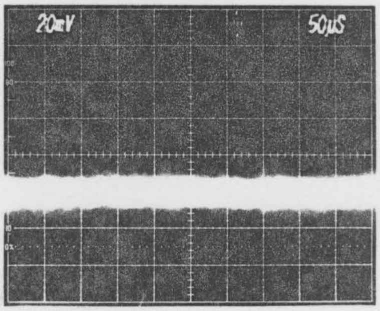

c) $V_{in}(V\text{-}F) = +10.0\ V_{D.C.}$

$V_{out} = +8.7\ V_{D.C.}$

$f = 415$ kHz

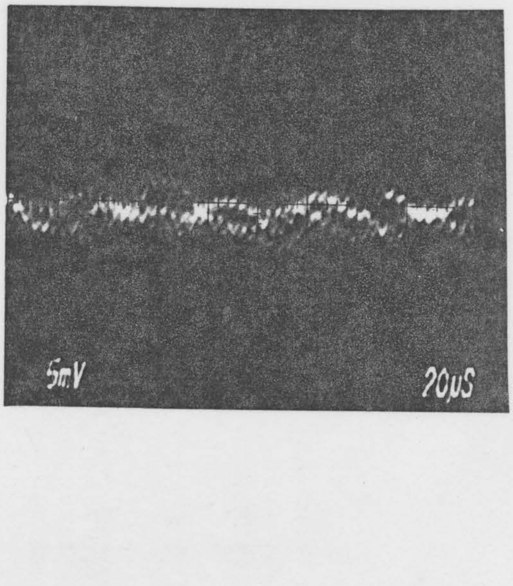

d) $V_{in} = +5.0\ V_{D.C.}$

$V_{out} = 0\ V_{D.C.}$

(Note: Expansion of both scale settings)

Note that high frequency noise has been filtered effectively leaving the uncertainty in V-F-V conversion as limiting noise.

Figure 16: Measured System Total Harmonic Distortion(THD)

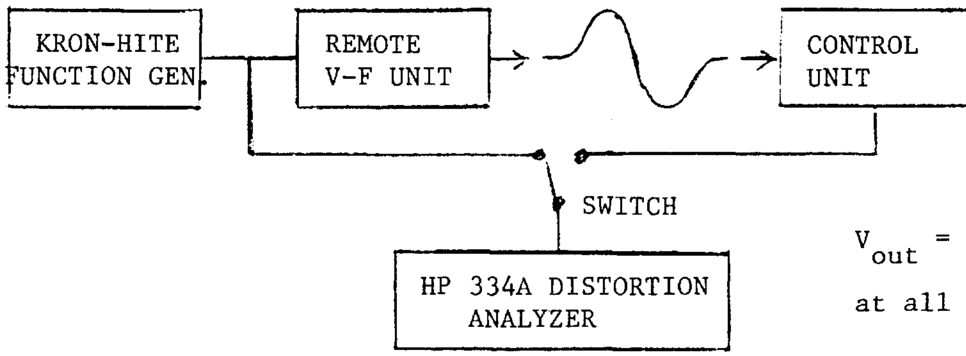

$V_{out} = 8V_{p-p}$ at all frequencies.

NOMINAL GAIN	MEASURED GAIN	TOTAL HARMONIC DIST. (%) 100Hz	1kHz	10kHz	Noise @ V_{out}:Vrms
x0.5	0.501	0.01	0.032	0.2	.0039
x1.0	1.001	0.015	0.033	0.210	.0039
x2.0	2.001	0.017	0.036	0.220	.0039
x5.0	5.013	0.015	0.043	0.240	.0039
x10.0	9.980	0.020	0.070	0.290	.0039
x20.0	19.771	0.023	0.124	0.410	.0039
x50.0	49.140	0.04	0.374	0.680	.0039

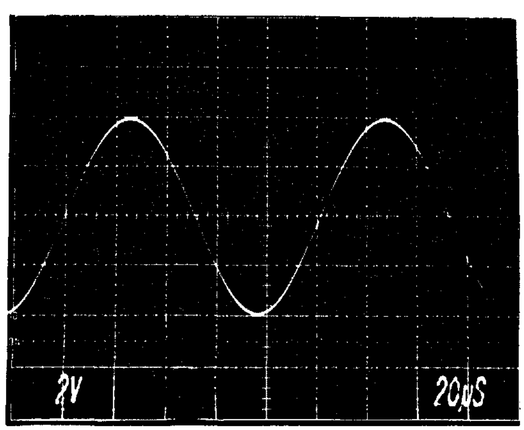

Output of System Under Worst Case Situation (x50.0 @ 10kHz).

Figure 17: Operational Amplifier Distortion Model

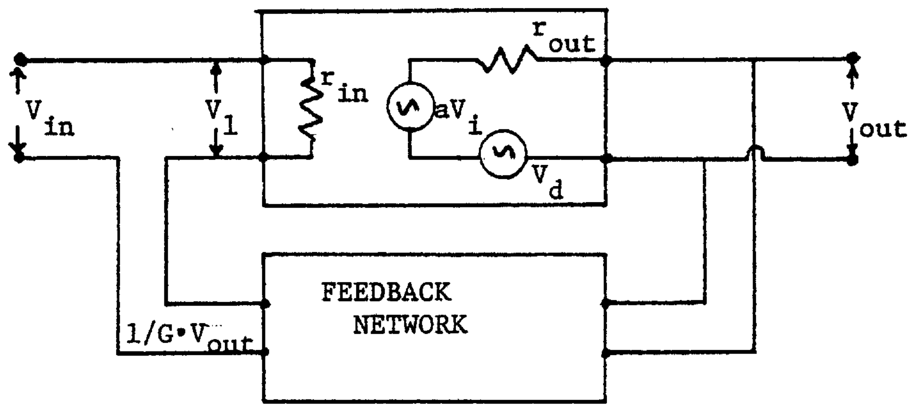

$$V_{out} = aV_1 + V_d = a(V_{in} + 1/G \cdot V_{out}) + V_d$$

$$= \frac{aV_{in}}{1-(a/G)} + \frac{V_d}{1-a/G} \approx GV_{in} - \frac{G}{a} \cdot V_d \text{ if } \frac{a}{G} \gg 1$$

$$= G \cdot V_{in} - V_d \cdot [A_o/G - 1]^{-1}$$

where: $G \equiv$ closed loop gain

$A_o(f) \equiv$ open loop gain at frequency f

$a(f) \equiv$ available excess gain at frequency f $= A_o(f) - G$

Typical Open Loop Gain vs frequency for MC4558

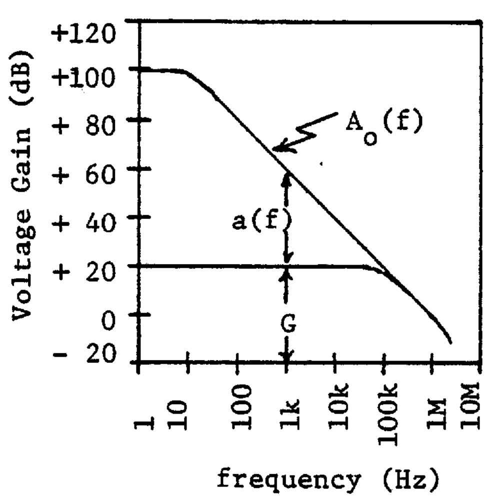

Table of Distortion Reduction Factor $(A_0/G - 1)^{-1}$ for MC4558

Gain (G)	frequency (Hz) 0-10	100	1k	10k
x0.5	$5x10^{-6}$	$5x10^{-5}$	$5x10^{-4}$	$5x10^{-3}$
x5.0	$5x10^{-5}$	$5x10^{-4}$	$5x10^{-3}$	$5x10^{-2}$
x50.0	$5x10^{-4}$	$5x10^{-3}$	$5x10^{-2}$	$5x10^{-1}$

Figure 18: System Bandwidth

LOW PASS FILTER REPSPONSE

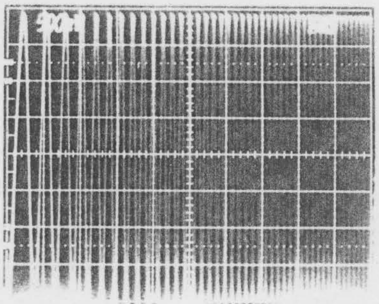
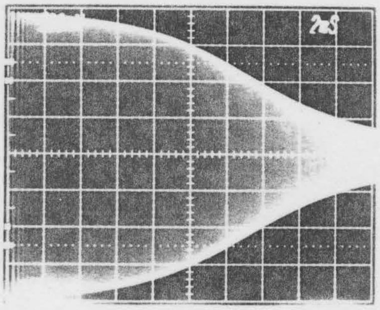

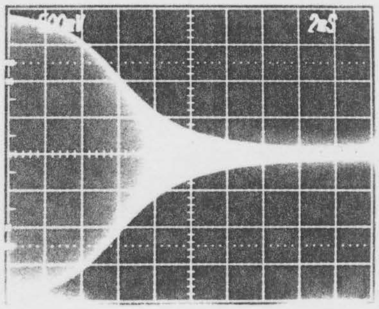

100Hz 4kHz 1kHz 40kHz 10kHz 90kHz

SYSTEM RESPONSE

small signal large signal

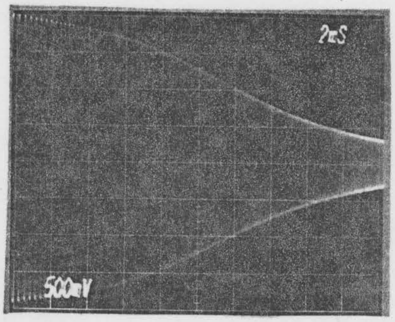

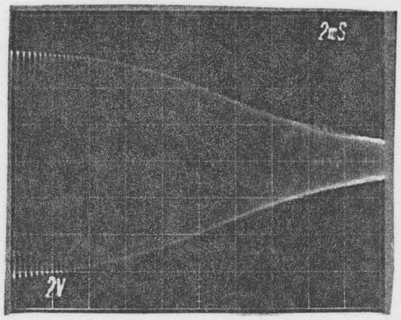

1kHz 40kHz 1kHz 40kHz

PULSE RESPONSE

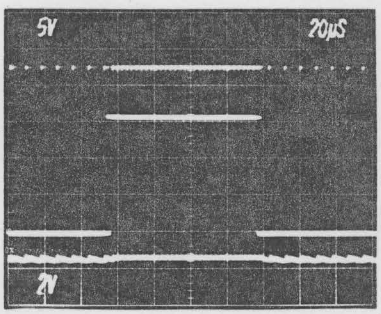

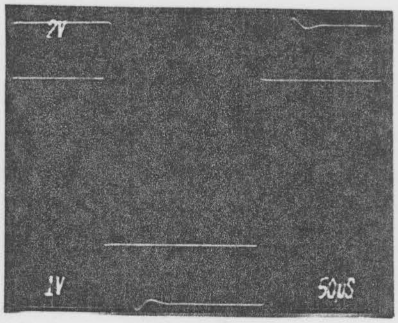

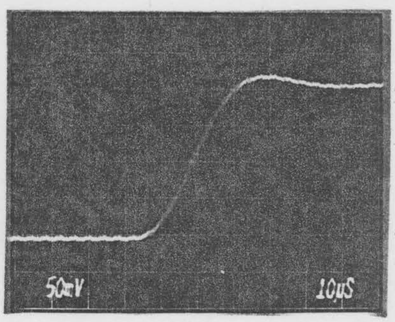

V-F Response to Pulse Large Signal Small Signal

Figure 19: Automatic Gain Switching

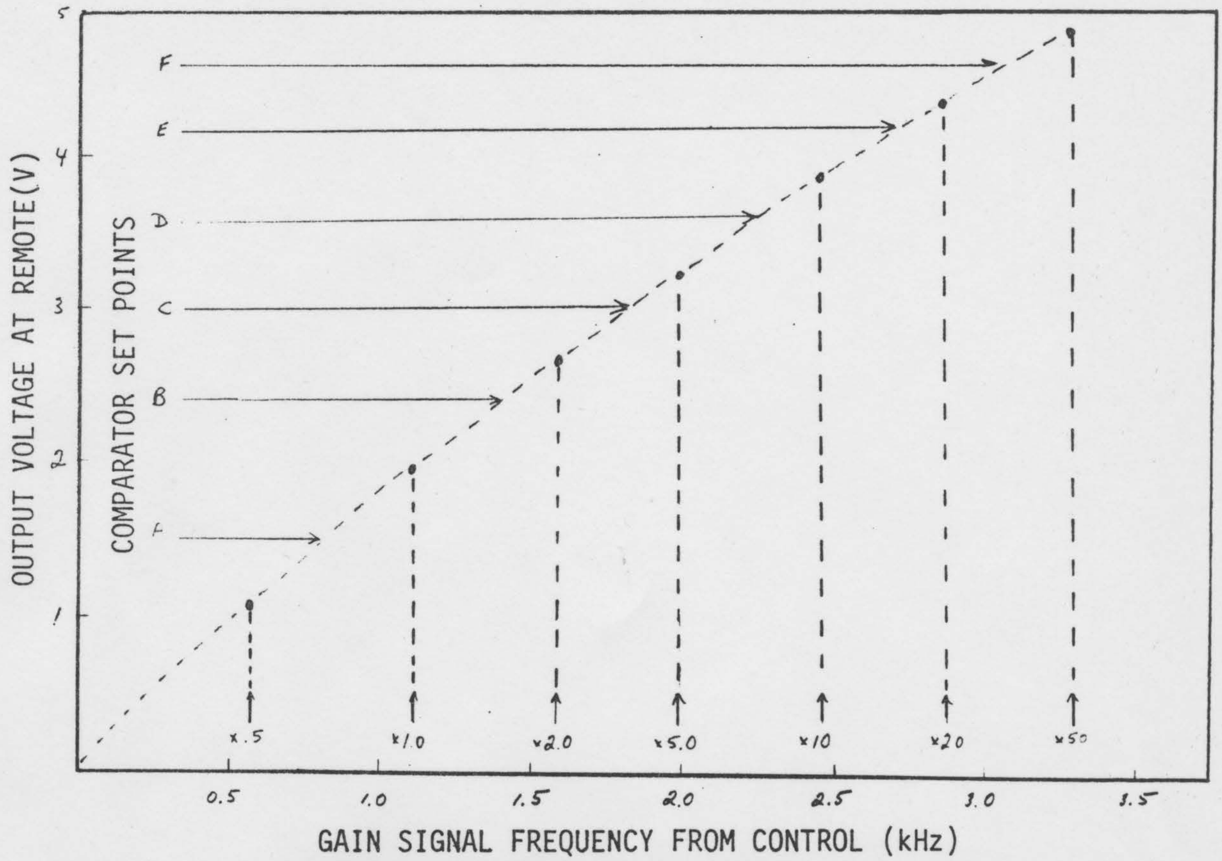

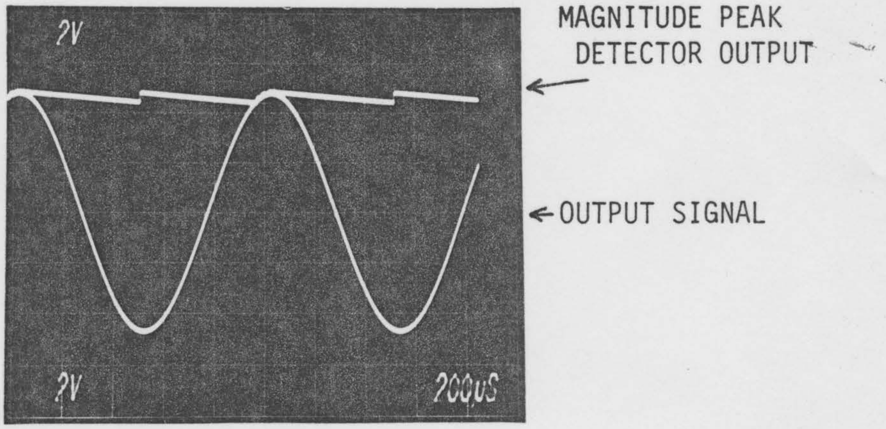

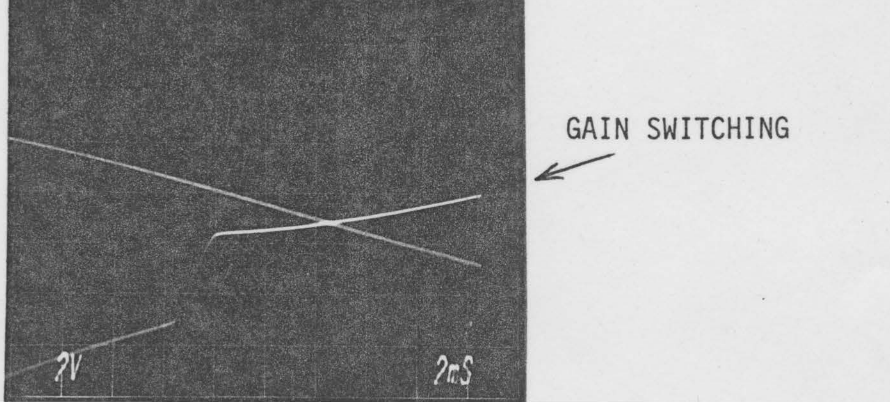

Figure 20: Table of System Specifications

POWER SUPPLY REQUIREMENTS			
CONTROL	+12V	@ 70mA (min)	195mA (max)
	-12V	@ 40mA (min)	60mA (max)
REMOTE	+12V	@ 55mA (min)	63mA (max)
	-12V	@ 12mA (max)	
V-F (alone)	+12V	@ 25mA (min)	32mA (max)

POWER SUPPLY REJECTION		ΔV_{out} (V_{out}=-8.3V)	ΔV_{out} (V_{out}=0V)	ΔV_{out} (V_{out}= +8.3V)
Control	$\Delta +V_{cc}=\pm 0.3V$	±.003	±0.001	± .007
	$\Delta -V_{cc}=\pm 0.3V$	±.001	±0.000	±.001
Remote & V-F alone	$\Delta +V_{cc}=\pm 0.1V$	±.007	±.006	±.005
	$\Delta -V_{cc}=\pm 0.2V$	±.000	±.000	±.000

Warmup time to within	0.4% = 0 min 0.1% = 8 min		
Input Voltage Range	Remote V-F Alone	-10 to +10 analog 0 to +10 analog	
DC Accuracy	±0.1% of full scale		
Output Ripple	7mV (max)	2mV (min)	
Output Load	4kΩ (min)		
Gain Levels (auto or manually selected)	x0.5, x1.0, x2.0, x5.0, x10.0, x20.0, x50.0.		
Bandwidth	DC to 17 kHz (-3dB)		
Total Harmonic Distortion (average)	100Hz 0.02%	1kHz 0.04%	10kHz 0.2%
Pulse Response	<8% overshoot 50 μsec settling time (1%)		

APPENDIX A

SIGNAL/NOISE CALCULATION

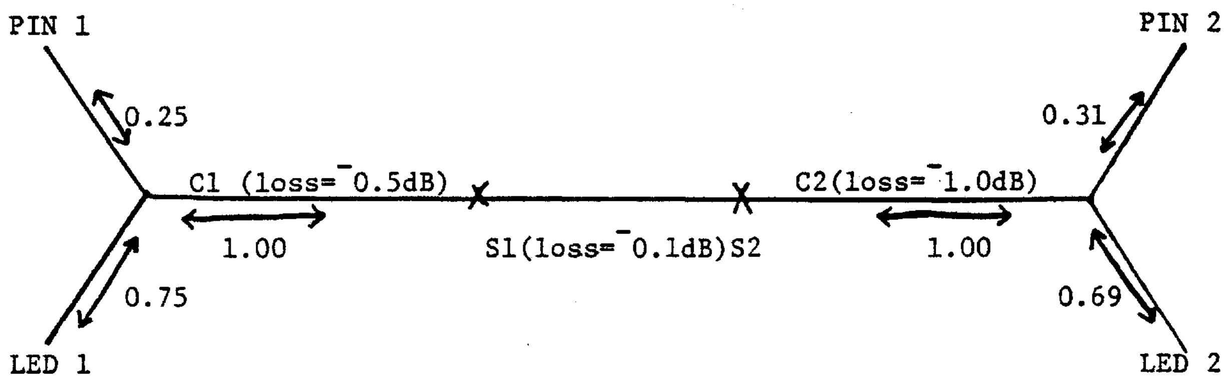

Assume LED 1 and LED 2 operated at equal output power levels and that the responsivities of the PIN's are equal. There is a 4% (-14dB) refelectivity at the fiber/air interface when terminated.

<u>Crosstalk between LED 1 and PIN 1:</u>

LED 1 $\rightarrow$ PIN 1 = -47dB

LED 1 $\rightarrow$ LED 2 $\rightarrow$ PIN 2 = Coupler 1 losses + fiber + splice losses + coupler 2 losses + reflection losses + C2 losses + fiber + splice + C1 losses

= -0.5dB - 1.3 - 0.1 - 1.6 - 1.0 - 14 - 1.0 -1.6 - 0.1 - 0.1 - 0.5 - 6dB - 1.8dB

= -29.7dB

LED 1 $\rightarrow$ PIN 2 $\rightarrow$ PIN 1 = -36.7dB

Net Crosstalk = $-28.8 - 2\alpha$ dB

Signal LED 2 $\rightarrow$ PIN 1 = $-11.1 - \alpha$ dB

$$\therefore S/N \Big|_{\text{PIN 1}} = (-11.1 - \alpha) - (-28.8 - 2\alpha) = 17.7 + \alpha \text{ dB.}$$

Worst Case: $\alpha = 0$ S/N = 17.7dB

APPENDIX A (con't)

Crosstalk between LED 2 and PIN 2:

L2 $\rightarrow$ PIN 2 = -46dB = 2.51×10^{-5}

L2 $\rightarrow$ L1 $\rightarrow$ PIN 2 = $-28.5 - 2\alpha$ dB

L2 $\rightarrow$ PIN 1 $\rightarrow$ PIN 2 = -37.7dB $- 2\alpha$ dB

Total Crosstalk = $-28.0 - 2\alpha$ dB

Signal at PIN 2 = $(-9.8 - \alpha)$dB

$$S/N \Big|_{PIN\ 2} = (-9.8 - \alpha) - (28.0 - 2\alpha) = 18.2 + \alpha \text{dB}$$

Measured Values: S/N (PIN 1) = -15.5dB
S/N (PIN 2) = -19.5dB

$I(\text{PIN 1}) = (9.72 \times 10^{-2} \times I_{LED\ 2} - 0.31)\mu A$ $\qquad$ I_{LED} in mA

$I(\text{PIN 2}) = (7.45 \times 10^{-2} \times I_{LED\ 1} - 0.22)\mu A$

Assuming I_{LED} = 50 mA, $I(\text{PIN 1}) = 3.5\mu A$ = 35mV (across $10k\Omega$)
$I(\text{PIN 2}) = 4.6\mu A$ = 46mV (across $10k\Omega$)

V_{NOISE} = 1.6 mV (max); Worst Case I_{DARK} = $(10\mu A)$ = $0.1 mV$.

Factor of 2 change in light output from -40 to +25°C and +25°C to 80°C

$\therefore$ set V_{trig} = 10mV.